NAVAL POSTGRADUATE SCHOOL

MONTEREY, CALIFORNIA

THESIS

CHARACTERIZATION OF ALUMINUM-MAGNESIUM ALLOY REVERSE SENSITIZED VIA HEAT TREATMENT

by

Kevin D. Gamble

September 2016

Thesis Advisor:	Kim Ngoc Tran
Co-Advisor:	Sarath Menon
Second Reader:	Terry McNelley

THIS PAGE INTENTIONALLY LEFT BLANK

REPORT DOCUMENTATION PAGE			Form Approved OMB No. 0704–0188
Public reporting burden for this collection of information is estimated to average 1 hour per response, including the time for reviewing instruction, searching existing data sources, gathering and maintaining the data needed, and completing and reviewing the collection of information. Send comments regarding this burden estimate or any other aspect of this collection of information, including suggestions for reducing this burden, to Washington headquarters Services, Directorate for Information Operations and Reports, 1215 Jefferson Davis Highway, Suite 1204, Arlington, VA 22202-4302, and to the Office of Management and Budget, Paperwork Reduction Project (0704-0188) Washington, DC 20503.			
1. AGENCY USE ONLY ***(Leave blank)***	**2. REPORT DATE** September 2016	**3. REPORT TYPE AND DATES COVERED** Master's thesis	
4. TITLE AND SUBTITLE CHARACTERIZATION OF ALUMINUM-MAGNESIUM ALLOY REVERSE SENSITIZED VIA HEAT TREATMENT			**5. FUNDING NUMBERS**
6. AUTHOR(S) Kevin D. Gamble			
7. PERFORMING ORGANIZATION NAME(S) AND ADDRESS(ES) Naval Postgraduate School Monterey, CA 93943-5000			**8. PERFORMING ORGANIZATION REPORT NUMBER**
9. SPONSORING /MONITORING AGENCY NAME(S) AND ADDRESS(ES) N/A			**10. SPONSORING / MONITORING AGENCY REPORT NUMBER**
11. SUPPLEMENTARY NOTES The views expressed in this thesis are those of the author and do not reflect the official policy or position of the Department of Defense or the U.S. Government. IRB Protocol number ____N/A____.			
12a. DISTRIBUTION / AVAILABILITY STATEMENT Approved for public release. Distribution is unlimited.			**12b. DISTRIBUTION CODE**

13. ABSTRACT (maximum 200 words)

This research explores a novel repair technique to reverse the sensitization of aluminum magnesium (Al-Mg) alloys. Al-Mg alloys can become sensitized when magnesium comes out of solution as a second phase, Al_3Mg_2, on the grain boundaries, eventually forming a continuous network and increasing susceptibility to intergranular stress corrosion cracking (SCC). Sensitized 5456 Al-Mg alloy samples removed from active Navy ships were metallographically characterized. These were compared to similar samples that were heat treated in order to reverse the sensitization effect. Both of these were also compared to "as wrought" 5456 aluminum. All samples were also tested for tensile strength and degree of sensitization using the ASTM G67 Nitric Acid Mass Loss Test (NAMLT).

Two heat treatment profiles were compared. Both of these profiles successfully reversed the sensitization effect, with similar performance. Heat treatment may have affected the tensile properties and negatively degraded the resulting microstructure by annealing the material. Therefore, more research is necessary to prove this technique's suitability for shipboard repair.

14. SUBJECT TERMS Reverse Sensitizing 5456 Aluminum Alloy			**15. NUMBER OF PAGES** 83
			16. PRICE CODE
17. SECURITY CLASSIFICATION OF REPORT Unclassified	**18. SECURITY CLASSIFICATION OF THIS PAGE** Unclassified	**19. SECURITY CLASSIFICATION OF ABSTRACT** Unclassified	**20. LIMITATION OF ABSTRACT** UU

NSN 7540–01-280-5500 Standard Form 298 (Rev. 2–89)
Prescribed by ANSI Std. 239–18

THIS PAGE INTENTIONALLY LEFT BLANK

Approved for public release. Distribution is unlimited.

CHARACTERIZATION OF ALUMINUM-MAGNESIUM ALLOY REVERSE SENSITIZED VIA HEAT TREATMENT

Kevin D. Gamble
Lieutenant Commander, United States Navy
B.S., University of Utah, 2002

Submitted in partial fulfillment of the
requirements for the degree of

MASTER OF SCIENCE IN MECHANICAL ENGINEERING

from the

NAVAL POSTGRADUATE SCHOOL
September 2016

Approved by: Kim Ngoc Tran
Thesis Advisor

Sarath Menon
Co-Advisor

Terry McNelley
Second Reader

Garth V. Hobson
Chair, Department of Mechanical and Aerospace Engineering

THIS PAGE INTENTIONALLY LEFT BLANK

ABSTRACT

This research explores a novel repair technique to reverse the sensitization of aluminum magnesium (Al-Mg) alloys. Al-Mg alloys can become sensitized when magnesium comes out of solution as a second phase, Al_3Mg_2, on the grain boundaries, eventually forming a continuous network and increasing susceptibility to intergranular stress corrosion cracking (SCC). Sensitized 5456 Al-Mg alloy samples removed from active Navy ships were metallographically characterized. These were compared to similar samples that were heat treated in order to reverse the sensitization effect. Both of these were also compared to “as wrought” 5456 aluminum. All samples were also tested for tensile strength and degree of sensitization using the ASTM G67 Nitric Acid Mass Loss Test (NAMLT).

Two heat treatment profiles were compared. Both of these profiles successfully reversed the sensitization effect, with similar performance. Heat treatment may have affected the tensile properties and negatively degraded the resulting microstructure by annealing the material. Therefore, more research is necessary to prove this technique’s suitability for shipboard repair.

THIS PAGE INTENTIONALLY LEFT BLANK

TABLE OF CONTENTS

I. INTRODUCTION 1
A. MOTIVATION 1
B. BACKGROUND 4
C. OBJECTIVES 12

II. EXPERIMENTAL METHODS 15
A. MATERIALS 15
B. SAMPLE PREPARATION 18
1. Microscopy Preparation 18
2. Tensile Test Specimen Preparation 20
3. Nitric Acid Mass Loss Test (NAMLT) Specimen Preparation 21
C. CHARACTERIZATION TECHNIQUES 22
1. Optical Microscope 22
2. Scanning Electron Microscope (SEM) 22
3. Energy Dispersive Spectroscopy (EDS) 23
4. Electron Backscatter Diffraction (EBSD) 23
5. Nitric Acid Mass Loss Test (NAMLT) 23
6. Tensile Test 25
7. Corrosion Test 26

III. RESULTS AND DISCUSSION 27
A. OPTICAL MICROSCOPE 27
B. SEM 28
C. EDS 33
D. EBSD 40
E. NAMLT 44
F. TENSILE TEST 45
G. CORROSION TEST 50

IV. CONCLUSIONS 53

V. FUTURE WORK 55

LIST OF REFERENCES 59

INITIAL DISTRIBUTION LIST 63

LIST OF FIGURES

Figure 1. Assorted Stock Photos Representing United States Navy Vessels Built using 5XXX Series Al-Mg. Source: [3]..... 2

Figure 2. A Worker Prepares to Replace a Stress Corrosion Cracking Damaged Ship Section. Source: [3]..... 4

Figure 3. SCC Triangle..... 4

Figure 4. Stress Corrosion Cracking, Exfoliation, and Hole Formation, Respectively, due to Sensitization. Source: [4]..... 5

Figure 5. IGSCC due to Al-Mg Sensitization. Source: [10]. 6

Figure 6. Al-Mg Phase Diagram. Adapted from [12]. 8

Figure 7. Microstructure of Non-sensitized and Partially Sensitized AA 5456-H116 (Obtained by Electron Backscatter Detector). 9

Figure 8. Manual Stabilization Treatment. Source: [9]. 10

Figure 9. Effect of Temperature on Al-Mg Alloys. Source: [9]. 11

Figure 10. NAMLT Results of Reverse Sensitized AA 5456-H116. Source: [9]. 12

Figure 11. “As-received” Non-sensitized AA5456 H116 Plate 15

Figure 12. Shipboard Plate “3A” 16

Figure 13. Shipboard Plate “6A” 16

Figure 14. Sensitized, Heat Treated AA5456. (a) Sensitized; (b) 249 °C (480 °F), 5 minutes; (c) 249 °C (480 °F), 10 minutes 17

Figure 15. Struers Secotom-10 Saw, Front View..... 18

Figure 16. Struers Secotom-10 Saw, Inside View 18

Figure 17. Specimen Orientations. Source: [17]. 20

Figure 18. Tensile Specimen Specifications. Source: [18]..... 21

Figure 19. (a) Tensile and (b) NAMLT Test Specimens 21

Figure 20. Nikon Epiphot 200 Optical Microscope..... 22

Figure 21. Zeiss Neon 40 Field Emission SEM 23

Figure 22. NAMLT Apparatus 24

Figure 23. Sartorius Model CP225D Digital Scale 25

Figure 24. Instron Model 4507 26

Figure 25. Rolling Direction Determination 27

Figure 26. SEM Backscatter Images of As-received and In-service (Shipboard) Plates (Obtained by Electron Backscatter Detector) 29

Figure 27. SEM Backscatter Images of Sensitized and Heat Treated AA 5456-H116 (Obtained by Electron Backscatter Detector) 30

Figure 28. SEM Backscatter Images of Heat Treatment Profiles (Obtained by Electron Backscatter Diffraction) 31

Figure 29. SEM Backscatter Image of 249°C / 5 Minute Profile (Obtained by Electron Backscatter Detector) 31

Figure 30. Secondary Electron Image of As-received AA5456 35

Figure 31. EDS Spectrum of As-received AA5456 35

Figure 32. Secondary Electron Image of Shipboard AA5456 36

Figure 33. EDS Spectrum of Shipboard AA5456 37

Figure 34. Secondary Electron Image of Heat Treated AA5456 38

Figure 35. EDS Spectrum of Heat Treated AA5456 38

Figure 36. Elemental Map of As-received AA5456 39

Figure 37. EBSD Scan of As-received AA 5456 41

Figure 38. EBSD Scan of Shipboard AA 5456 42

Figure 39. Stress-Strain Equations 46

Figure 40. As-received AA 5456 Stress Strain Curve 46

Figure 41. Shipboard Baseline AA 5456 Stress Strain Curve 47

Figure 42. Adjacent AA 5456 Stress Strain Curve 48

Figure 43. AA5456 Heat Treated 249 °C/5 Min Stress Strain Curve 48

Figure 44. Effect of Temperature on Al-Mg Alloys. Adapted from [9]..... 56

Figure 45. HDPL Array. Adapted from [25]. 57

THIS PAGE INTENTIONALLY LEFT BLANK

LIST OF TABLES

Table 1. Chemical Composition of 5xxx series Al-Mg Alloys. Adapted from [6], [22]. 34

Table 2. Chemical Composition of As-received AA5456 (Obtained by EDS) 34

Table 3. Chemical Composition of Shipboard AA5456 (Obtained by EDS) 36

Table 4. Chemical Composition of Heat Treated AA5456 37

Table 5. NAMLT Results 44

Table 6. As-received AA 5456 Tensile Test Results 47

Table 7. Shipboard Baseline AA 5456 Tensile Test Results 47

Table 8. Adjacent AA 5456 Tensile Test Results 48

Table 9. AA5456 Heat Treated 250 °C/5 Min Tensile Test Results. 49

THIS PAGE INTENTIONALLY LEFT BLANK

LIST OF ACRONYMS AND ABBREVIATIONS

AA	aluminum alloy
ANSI	American National Standards Institute
ASM	American Society for Metals
ASTM	American Society for Testing and Materials
β-phase	beta phase
BSD	backscatter detector
CG	cruiser, guided missile
CVN	aircraft carrier, fixed-wing, nuclear
°C	degrees Celsius
EBSD	electron backscatter diffraction
EDS	energy dispersive spectroscopy
FFG	fast frigate
IGC	intergranular corrosion
IGSCC	intergranular stress corrosion cracking
K_{1scc}	Stress corrosion cracking threshold
LCAC	landing craft, air cushion
LCS	littoral combat ship
LED	light emitting diode
LHA	landing, helicopter, assault
LRA	L. Raymond & Associates
min	minute
mm	millimeter
MPa	mega pascal
NAMLT	nitric acid mass loss test
NAVSEA	Naval Sea Systems Command
NSWC CD	Naval Surface Warfare Center, Carderock Division
SCC	stress corrosion cracking
SEM	scanning electron microscope
SSC	ship to shore connector

STEM	scanning transmission electron microscopy
TEM	transmission electron microscope
UTS	ultimate tensile strength
YS	yield strength

ACKNOWLEDGMENTS

I would like to thank my thesis advisors, Doctors Kim Ngoc Tran, Sarath Menon, and Terry McNelley. They provided exceptional guidance and support throughout my research and coursework. They are the true experts in this field; I feel I have just scratched the surface.

I would also like to thank the dedicated Naval Postgraduate School staff for assisting with material preparation and laboratory support. Specifically, Doctor Chanman Park, Mr. John Mobley, and Mr. Levi Owen were instrumental in this regard. Special thanks to Mr. Nathan Korinchack of Naval Surface Warfare Center, Carderock Division, for assisting me with tensile test data techniques.

I especially want to think my family. My wife, Jane, and my young son, Kayden, endured many long days without Daddy during this process. Their love and support allowed me to pursue this research on behalf of the United States Navy and our great nation. Without them, none of this could have been possible.

THIS PAGE INTENTIONALLY LEFT BLANK

I. INTRODUCTION

A. MOTIVATION

Aluminum alloys are attractive ship-building materials. They are lightweight, corrosion resistant, often weldable, machineable, abundant, and relatively inexpensive. Alloying of aluminum with elements such as magnesium favorably improves material properties over pure aluminum. Naval ships use primarily two particular Aluminum Magnesium (Al-Mg) alloys: AA5456 and AA5083.[1] The primary difference between these two alloys is the Mg content, being 4.7–5.5% Mg and 4.0–4.9% Mg, respectively, making AA5456 a stronger alloy [1]. Magnesium content at these percentages is high compared to other Al-Mg alloys.

The 5XXX series Al-Mg are non-heat treatable alloys that rely on solid solution strengthening and strain hardening as strengthening mechanisms. By comparison, AA6061, a heat treatable alloy, has higher yield strength prior to welding, but lower yield strength than 5XXX series Al-Mg alloys following welding. This makes 5XXX series Al-Mg alloys the more attractive choice for shipbuilding. Specifications for “marine grade” aluminum alloys are outlined in ASTM B928 Standard Specification for High Magnesium Aluminum—Alloy Sheet and Plate for Marine Service and Similar Environments [1].

According to the American National Standards Institute (ANSI), marine-grade 5XXX series Al-Mg alloys are made to temper designations H116 (strain hardened) or H321 (thermally stabilized) [2]. Research presented in this paper will focus on AA5456-H116, although findings are also applicable to other marine-grade alloys of comparable magnesium content.

For active ships and craft that use either AA5456 or AA5083, refer to Figure 1.

[1] AA5454 and AA5086 are also used to a lesser extent.

- Nimitz class aircraft carrier (CVN-68 class)
- Ticonderoga class guided missile cruiser (CG-47 class)
- America class Landing Helicopter Assault ship (LHA-6 class)
- Freedom and Independence Littoral Combat Ship (LCS-1 and LCS-2 classes)
- Spearhead class Joint High Speed Vessel (JHSV-1 class)
- Landing Craft, Air Cushion (LCAC)
- Ship to Shore Connector (SSC) (LCAC replacement)

Figure 1. Assorted Stock Photos Representing United States Navy Vessels Built using 5XXX Series Al-Mg. Source: [3].

The FFG-7 class also used 5XXX series Al-Mg alloys in their superstructures, but the class has been retired. The twenty-two active CG-47-class ships have long remaining service lives, provided expensive modernization and repair programs continue. A large part of these ships' operating expense is the repair of their aluminum superstructure, which is prone to stress corrosion cracking (SCC). The LCS, JHSV, SSC, and LHA-6 classes are still near the beginning of their service lives, and the carrier is the cornerstone of the U.S. fleet.

The U.S. Navy spends approximately $5 million per ship per year in maintenance due to SCC of Al-Mg alloys and $2.5 billion annually in total Navy ship corrosion-related costs [4], [5]. As the Navy builds more ships with Al-Mg alloys, there is a need to reduce repair costs either by developing lower cost repair techniques, or preventing damage from occurring, or both. Current repair techniques involve cutting out sections of the SCC-affected structure and welding in new material, as shown in Figure 2. This process is expensive because of the material and the skilled welders required to perform the repair. The worker has cut out damaged deck plate and has cleaned and prepared the surface for welding a new insert plate. This is a messy and invasive procedure. The time required to effect repairs lowers operational availability of the ship being repaired, and decreases readiness of the fleet. There is a need to develop a new repair technique that is faster, less expensive, and less intrusive than cutting and welding new aluminum sections on every ship.

Figure 2. A Worker Prepares to Replace a Stress Corrosion Cracking Damaged Ship Section. Source: [3].

B. BACKGROUND

Stress corrosion cracking of aluminum is a preventable ailment. SCC requires three elements acting together in order to occur. Those elements are shown in Figure 3.

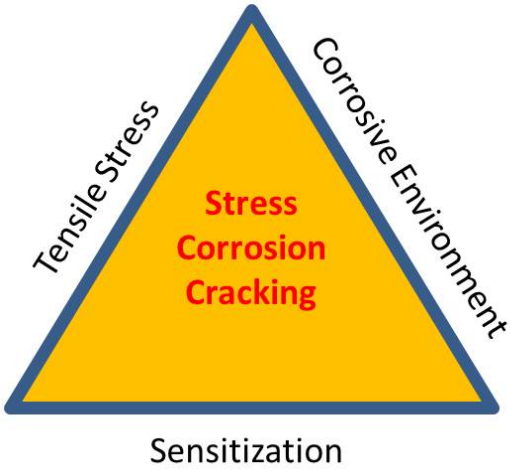

Figure 3. SCC Triangle

Navy ships spend their existence exposed to seawater, a corrosive environment. The rough nature of the sea interacting with the ship's rigid body of interconnected fixtures results in tension applied to those fixtures. The remaining element of the SCC Triangle, susceptibility, depends on the material. In the case of Al-Mg alloys, these are selected because they are not initially susceptible to SCC. They are lightweight, strong enough to withstand the tensile forces to which they are intended to be exposed, and they are resistant to seawater corrosion due to the active aluminum oxide layer that readily forms on their surface, preventing exposure to the underlying material [6].

Al-Mg alloys become susceptible, however, if they become "sensitized." Once sensitized, all three elements are present for SCC of the Al-Mg alloys to occur. Over time, the material may crack and/or exfoliate. SCC in Al-Mg alloys is intergranular in nature [7]. The term intergranular stress corrosion cracking (IGSCC) is often used when discussing SCC in aluminum alloys. Shown in Figure 4, from left to right, are the effects of cracking, exfoliation, and formation of a significant-sized hole.

Figure 4. Stress Corrosion Cracking, Exfoliation, and Hole Formation, Respectively, due to Sensitization. Source: [4].

Since ships are inherently exposed to a corrosive environment and tensile stresses cannot be completely eliminated, sensitization must be controlled in order to prevent SCC.

Sensitization occurs when Mg rich β-phase (Al_3Mg_2) precipitates at grain boundaries [7]. The degree to which the material is sensitized increases with increased β-phase precipitate formation. Because magnesium is electrochemically anodic compared to aluminum, this β-phase will preferentially corrode, allowing IGSCC. Sensitization reduces the material's crack resistance. As a result, cracks may form at stresses that are well below the yield stress of the material [8].

The sensitization phenomenon is illustrated in Figure 5. We begin with a new AA 5XXX plate on the left. When exposed to elevated temperature over time (years, in this case) magnesium diffuses from within the grain crystal to form a β-phase precipitate at the grain boundary, in the form of Al_3Mg_2. The β-phase precipitates can form a continuous, anodic and brittle film on the grain boundaries. Once the grain boundary precipitates becomes continuous, or nearly continuous, the material is considered sensitized. When this sensitized material is exposed to tension in this susceptible state, it is prone to IGSCC. Discontinuous β-phase precipitate at the grain boundaries will not result in SCC [9].

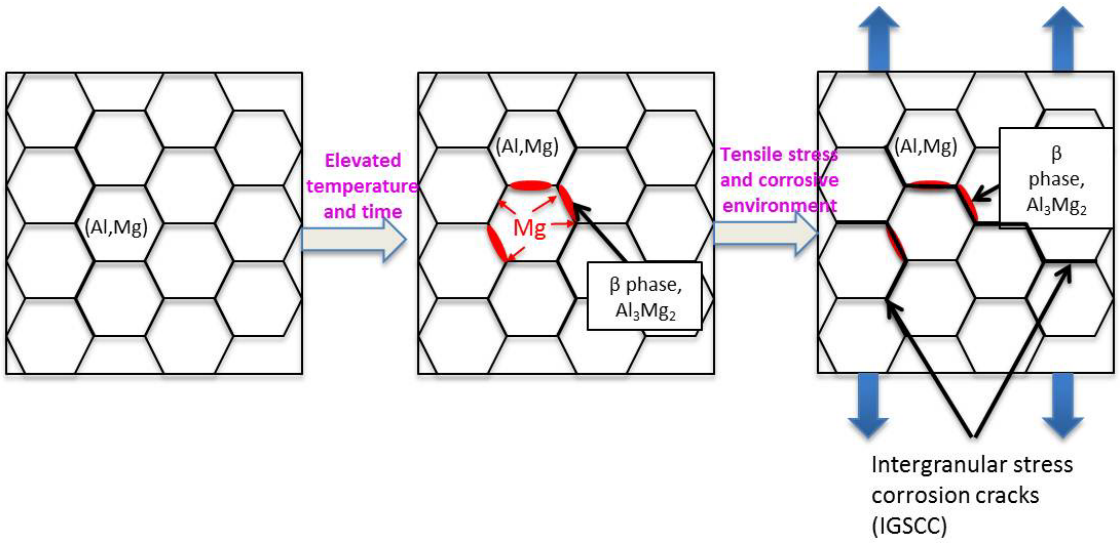

Figure 5. IGSCC due to Al-Mg Sensitization. Source: [10].

Sensitization of 5XXX series Al-Mg generally occurs at service temperatures above 65°C (150°F), which can be reached upon exposure to direct sunlight or in locations near engine compartments [10]. Sensitization has been known to occur at temperatures as low as 50°C (122°F) when exposure is prolonged [11]. This phenomenon can be understood considering the Al-Mg phase diagram in Figure 6. AA5456 has 4.7–5.5 wt% Mg. Locally, this percentage can be lower. To some extent lower Mg content lowers the temperature at which material will become sensitized. Sensitization only occurs in Al-Mg alloys with more than 3 wt% Mg [7], [11]. The microstructures of as-received (non-sensitized) material and in-service material cut from an active Navy Cruiser (partially sensitized) are shown in Figure 7. The qualitative assessment of sensitization can be seen in the darker, more continuous grain boundaries formed by β-phase precipitate, in the in-service material.

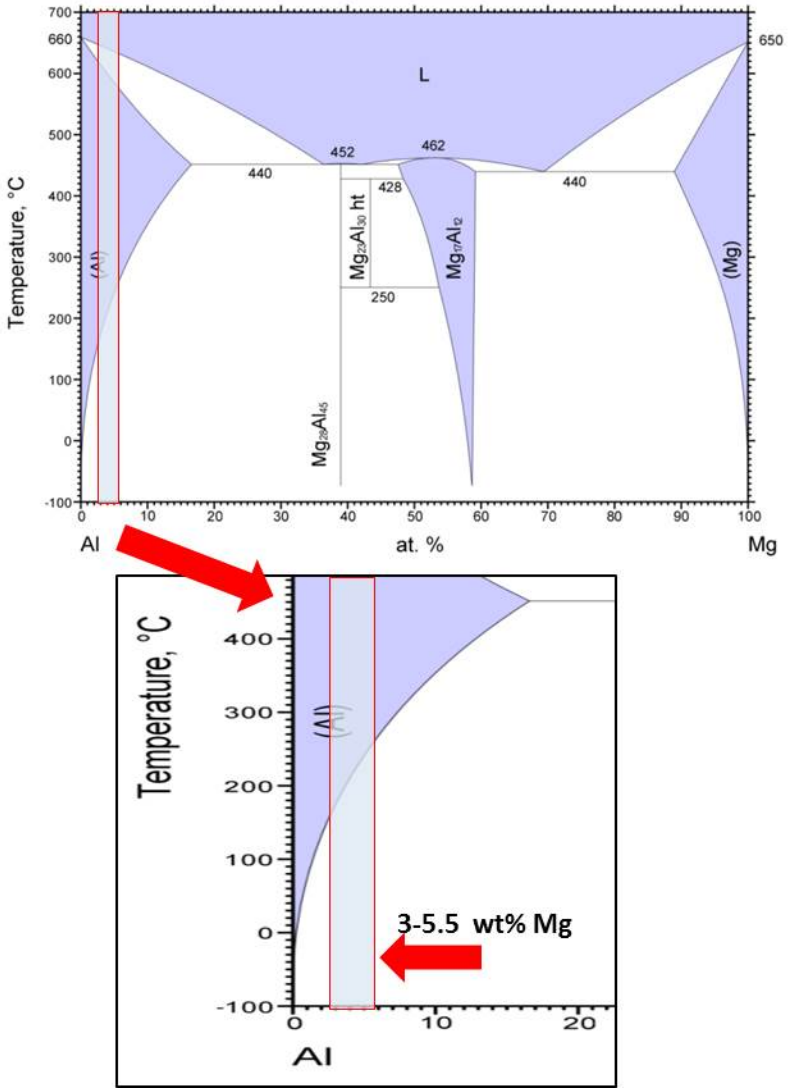

Figure 6. Al-Mg Phase Diagram. Adapted from [12].

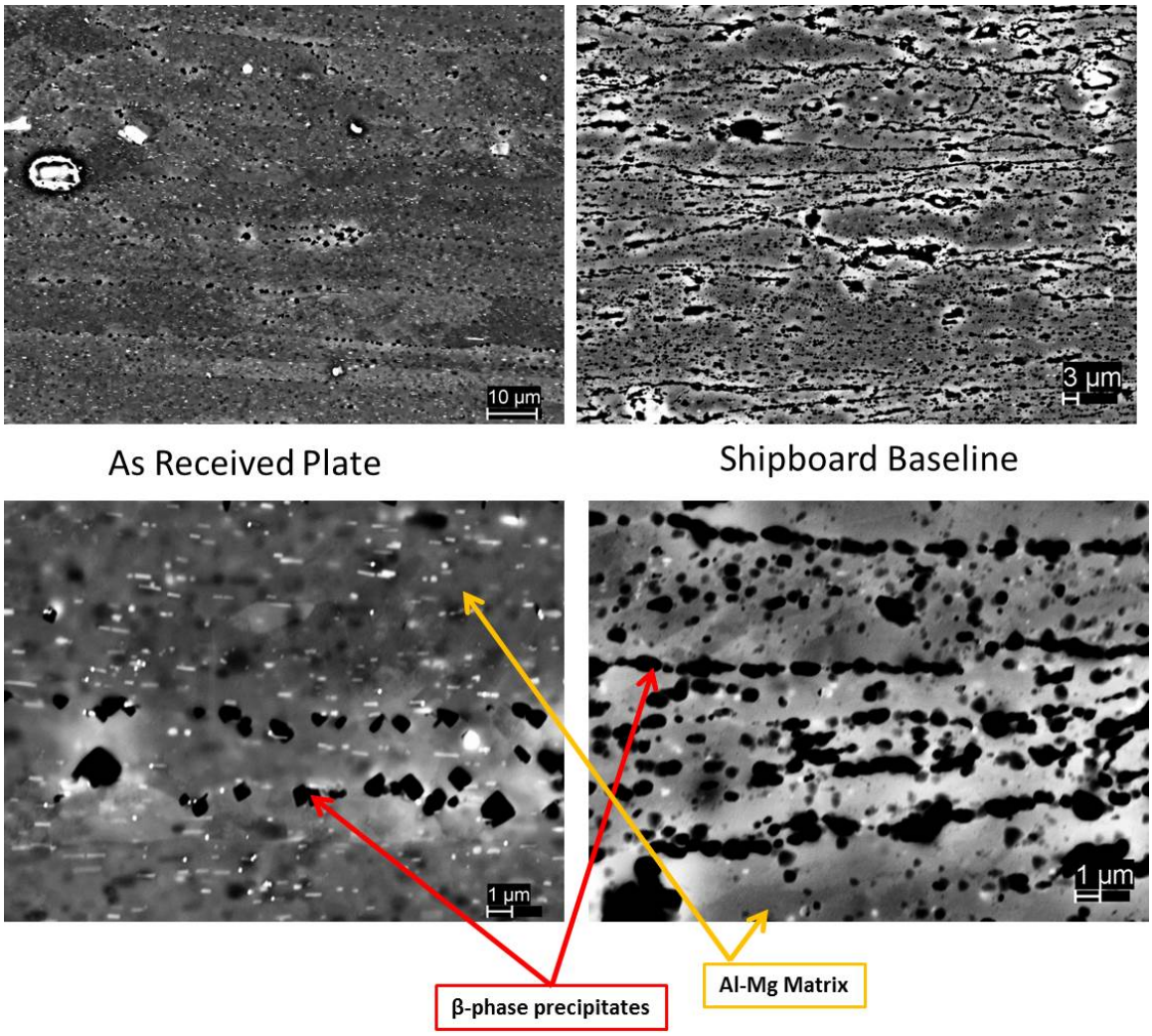

Figure 7. Microstructure of Non-sensitized and Partially Sensitized AA 5456-H116 (Obtained by Electron Backscatter Detector).

Sensitization of AA5456 has been successfully reversed in the laboratory by L. Kramer et al. in 2007 [9]. Further experiments funded by the Office of Naval Research (ONR) have demonstrated that reverse-sensitized AA5456 also recovers resistance to stress corrosion cracking following reverse sensitization heat treatment [13]. An evolutionary next step is the optimization of a reverse sensitization heat treatment time-temperature profile and up-scaling of the process to be used in-situ.

Kramer et al. studied the viability of reverse sensitization and found it to be effective [9]. They used a portable ceramic pad heating panel similar to the one shown in Figure 8.

Figure 8. Manual Stabilization Treatment. Source: [9].

This technique is analogous to the stabilization heat treatment done in the manufacturing process of rolled Al-Mg plate. Illustrated in Figure 9, Kramer et al. applied a heat treatment following cold work (rolling). This heat treatment is performed at a temperature below that which would result in the material being annealed, allowing it to retain the increased strength from cold work. This is a narrow temperature band. If the temperature is too low, sensitization is accelerated by β-phase precipitates forming in the supersaturated solid solution matrix [9]. If the temperature is too high, β-phase precipitates will dissolve into the solution but the material will be annealed, reducing the strength gained by the manufacturer's strain hardening [9]. It was also verified that the material could be sensitized again when exposed to elevated temperatures, as shown in Figure 10.

Kramer et al. identified the temperature range of 240–280 °C, applied for time periods of as little as 10 minutes, as showing promise for use as a technique to reverse sensitization. Using a Nitric Acid Mass Loss Test (NAMLT) [14] to assess the degree of sensitization, this heat treatment technique was verified to decrease the degree of sensitization.

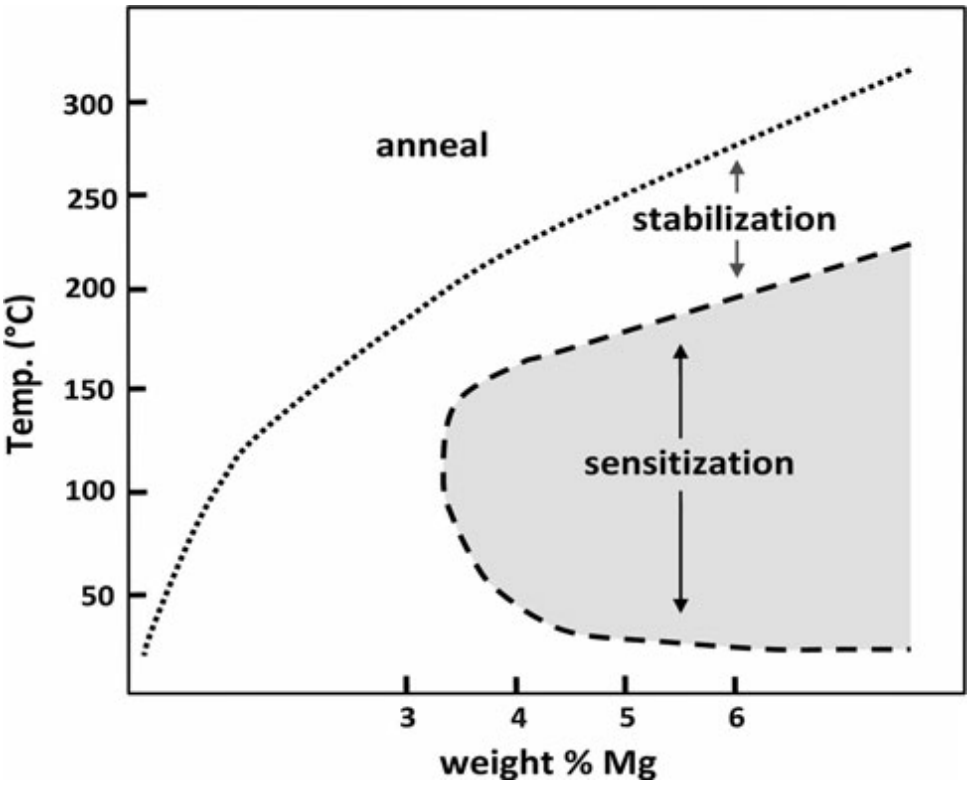

Figure 9. Effect of Temperature on Al-Mg Alloys. Source: [9].

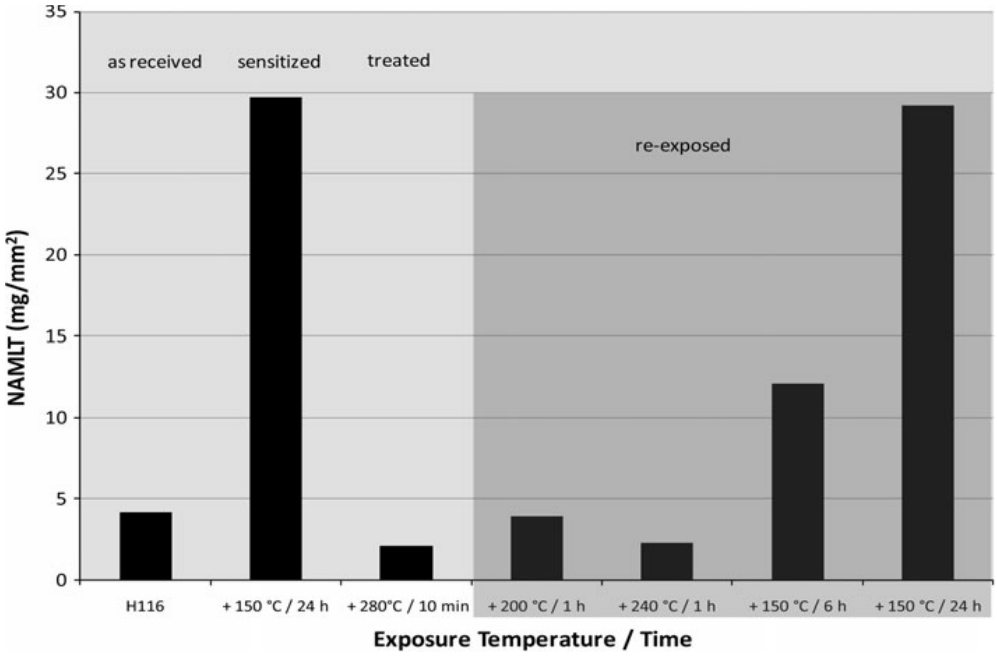

Figure 10. NAMLT Results of Reverse Sensitized AA 5456-H116. Source: [9].

C. OBJECTIVES

The objective of this thesis is to characterize AA5456 in three sensitization conditions, as-received (non-sensitized), naturally sensitized, and reverse sensitized. This characterization will consider specific heat treatment time-temperature profiles applied by an induction heating apparatus in order to select optimal time-temperature profile for potential use in-situ. Characterization will involve three specific goals:

(1) *Determine the microstructural characteristics of sensitized and reverse sensitized Al-Mg.* Microstructure analysis will be conducted using optical microscope, scanning electron microscope (SEM), energy dispersive spectroscopy, and electron backscatter diffraction (EBSD) techniques.

(2) *Determine results of mechanical and corrosion tests of sample material.* Tensile tests and ASTM G67 Standard Test Method for Determining the Susceptibility to Intergranular Corrosion of 5XXX Aluminum Alloy by Mass Loss

After Exposure to Nitric Acid (NAMLT) [14] will be conducted, and third-party stress corrosion cracking threshold (K_{1scc}) test data will be considered.

(3) *Determine what heat treatment procedure is most efficient for reversing sensitization (temperature, time).* This will be determined by comparing data from sensitized and reverse sensitized AA5456 samples.

THIS PAGE INTENTIONALLY LEFT BLANK

II. EXPERIMENTAL METHODS

A. MATERIALS

As-received (non-sensitized) plates were procured from Aleris, shown in Figure 11. They measured approximately 9.5 mm thick. The rolling direction was obvious by visual inspection in the direction of the longest measurement. A portion of these were subjected to heating in order to sensitize them. A specimen heated at 100 °C for 7 days was verified as being sensitized and characterized for comparison to the other plates. Though it is not from the exact plate subjected to heat treatment, the resulting sensitized microstructure was indicative of the microstructure that the sensitized plate had prior to heat treatment.

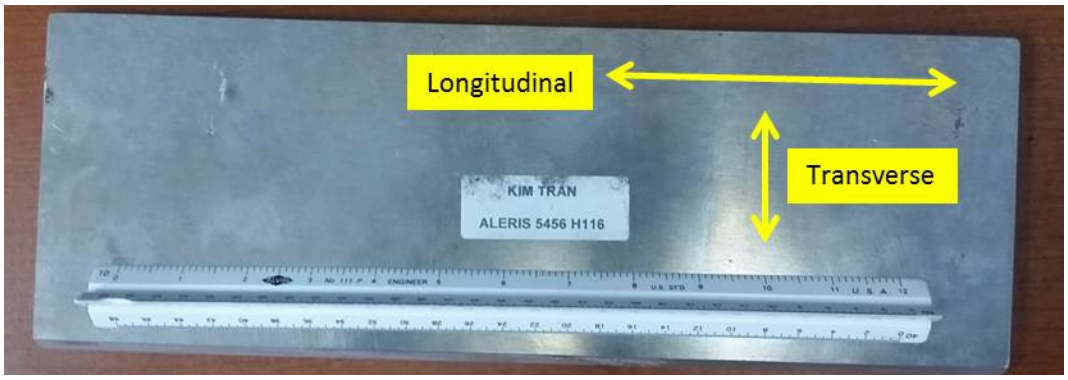

Figure 11. "As-received" Non-sensitized AA5456 H116 Plate

Plates cut from active Ticonderoga-class guided missile cruisers (CGs) were provided by the Naval Surface Warfare Center, Carderock Division (NSWCCD). Three plates were provided, but only two were subjected to characterization due to extreme deterioration of the third plate. The two plates used for characterization were labeled "3A" and "6A," shown in Figures 12 and 13. This nomenclature is indicated on following test results where these plates were used. Their thickness varied slightly from 6.21 mm to 6.67 mm (around 0.25 inches). These plates had been on ships that had seen an unknown cycle of painting-stripping-repainting, so some variation was expected.

The exact age and range of exposed environments is unknown on these plates, but guided missile cruisers have been built and deployed since 1983 [15]. Given the age of even the newest CG, it was assumed that these plates would show some degree of sensitization. Plate “6A” was labeled to indicate that it had come from the USS *Monterey* (CG-61), which was commissioned in 1990 and has endured several deployments to the Persian Gulf [16], where temperatures exceed those required for sensitization. CG-61 is homeported in Norfolk, VA.

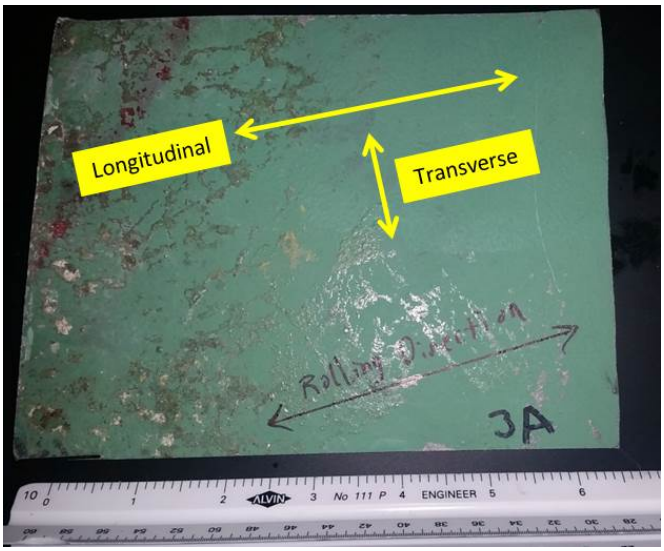

Figure 12. Shipboard Plate “3A”

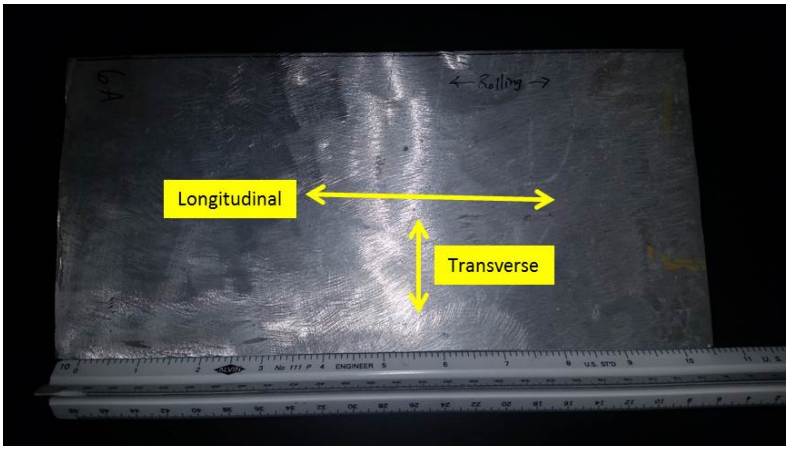

Figure 13. Shipboard Plate “6A”

Another plate cut from an active CG was subjected to two different heat treatment profiles. Shown in Figure 14, three sample areas were examined from this plate—non-heat treated area, and areas heat treated at 249 °C (480 °F) for 5 minutes, and 249 °C (480 °F) for 10 minutes, respectively. NAMLT was conducted prior to heat treatment to confirm this material as sensitized.

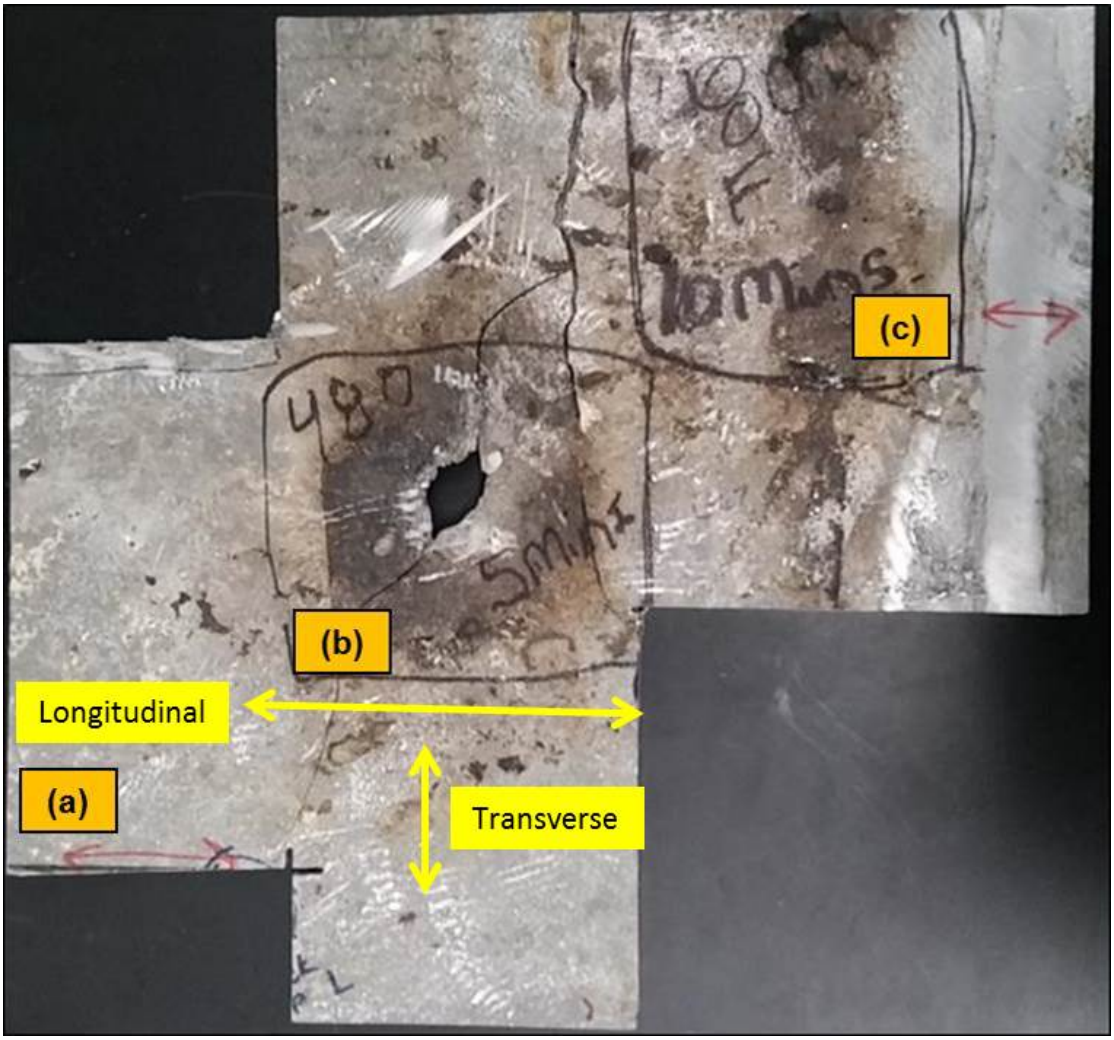

Figure 14. Sensitized, Heat Treated AA5456. (a) Sensitized; (b) 249 °C (480 °F), 5 minutes; (c) 249 °C (480 °F), 10 minutes

B. SAMPLE PREPARATION

1. Microscopy Preparation

Samples were cut into smaller sections using a band saw and were further cut into rectangles measuring approximately 20 mm x 6 mm using a water-cooled Struers Secotom-10 saw, with an abrasive cutting wheel. The machine's aluminum cutting settings were 3000 RPM wheel speed and 1.0 mm/second feed speed. Two specimens were cut from each plate, in the longitudinal and transverse directions.

Figure 15. Struers Secotom-10 Saw, Front View

Figure 16. Struers Secotom-10 Saw, Inside View

For ease of polishing, specimens were then mounted in molds using a Buehler SimpliMet 2 mounting press. The mounting material used was Buehler ProbeMet conductive molding compound. The specimens were loaded onto a

Buehler AutoMet 2 polisher and polished. Settings for all steps were five pounds' force at 150 RPM with a constant water flow as lubricant/coolant.

Polishing regimen:

- 120 grit aluminum oxide paper for 10 minutes.
- 220 grit aluminum oxide paper for 20 minutes.
- 500 grit aluminum oxide paper for 20 minutes.
- 1200 grit aluminum oxide paper for 10 minutes.
- #2000 silicon carbide paper for 20 minutes.
- #4000 silicon carbide paper for 20 minutes.
- 1 µm Alumina (Al_20_3) micropolish on polishing cloth for 20 minutes.
- 0.05 Alumina (Al_20_3) micropolish on polishing cloth for 20 minutes.

Specimens were then polished on a Buehler VobroMet 2 vibratory polisher for two hours using 0.05 µm Alumina. Specimens were then hand polished for 1 minute on the AutoMet using a clean polishing cloth and water. They were then rinsed with distilled water, methanol, and heated to dry. Specimens were then removed from their molds to conduct the next polishing step. The molds were crushed in a vise, carefully removing the specimen without damage.

Specimens were then electro-polished with a Buehler ElectroMet 4 in 10% Perchloric acid-90% ethanol electrolyte held at -40˚C and at 15V. Shipboard specimens were polished for 30 seconds while as-received specimens were polished for 20 seconds. Because the electro-polishing procedure removes surface particles from the material being polished, a shorter polishing time was used on material with a higher degree of sensitization in order to lessen removal of β-phase particle, leaving them in place for visual microscopic observation. Following polishing, specimens were quickly placed in ethanol and then dried with a heated blower. Finally, specimens were lightly etched with Keller's solution for a few seconds. All specimens were stored in a vacuum chamber.

For determination of rolling direction, the plates were viewed under optical microscope with no prior preparation. This avoided disturbing the as-manufactured surface and kept the rolling direction readily visible. Possible orientations for specimen preparation are shown in Figure 17.

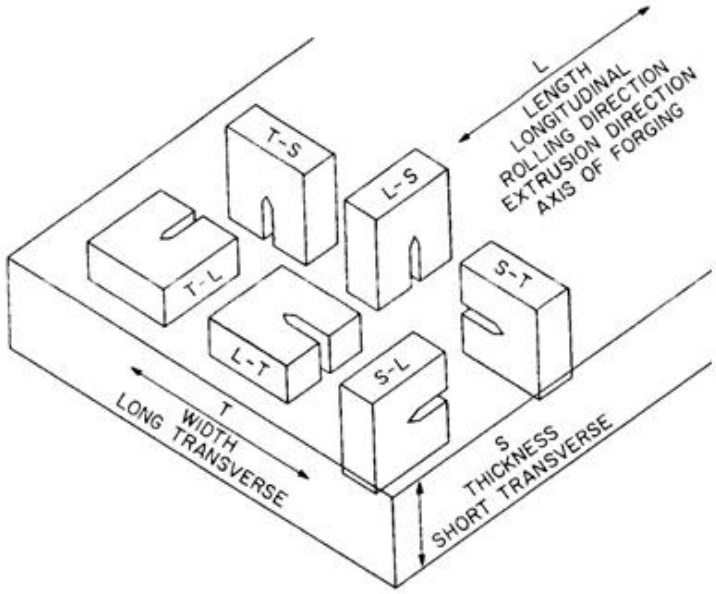

Figure 17. Specimen Orientations. Source: [17].

2. Tensile Test Specimen Preparation

Specimens were prepared in accordance with ASTM B557M [18] using the specifications for flat sub-sized specimens, illustrated in Figure 18 and shown in Figure 19a. The sub-size specimens were used due to the small amount of material available for testing. These were flat specimens with a 32 mm initial gage length and 100 mm overall length. Both the tensile and NAMLT specimens were fabricated on a mill with Trim Sol ® cooling liquid applied during fabrication. Care was taken to avoid high temperature during the fabrication process which could have affected test results and microstructure by annealing the material.

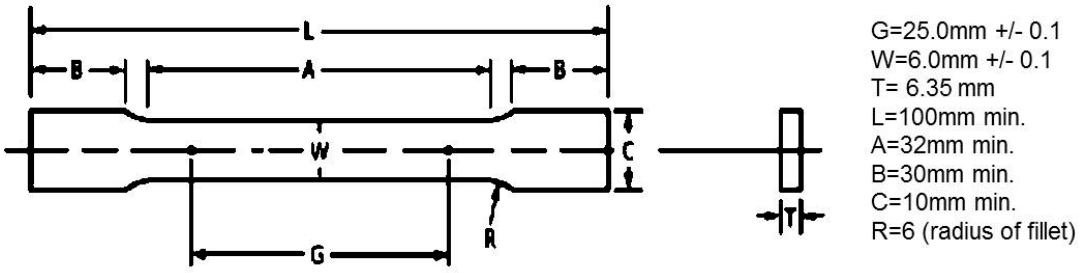

Figure 18. Tensile Specimen Specifications. Source: [18].

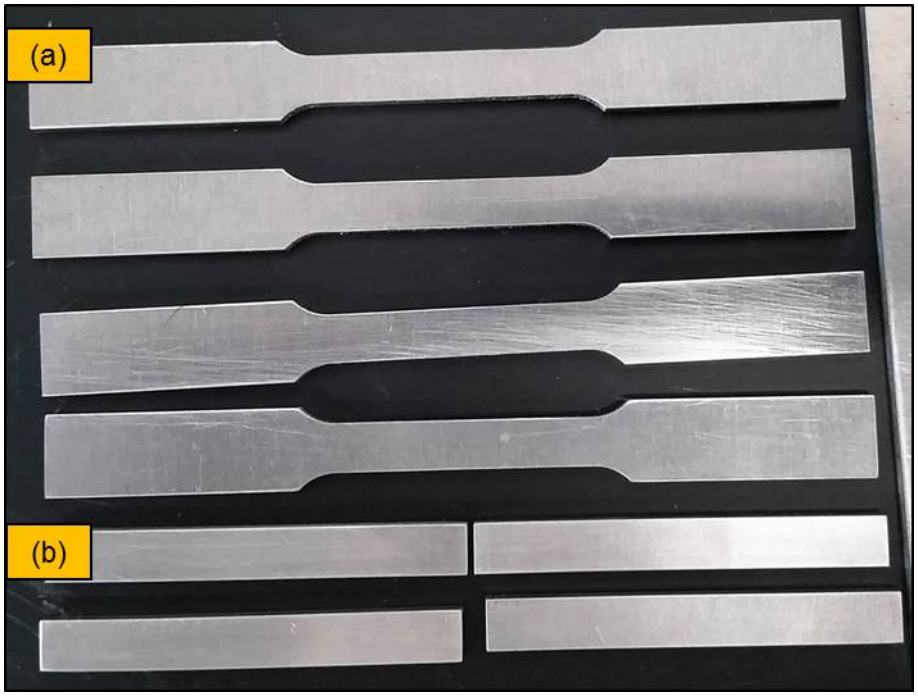

Figure 19. (a) Tensile and (b) NAMLT Test Specimens

3. Nitric Acid Mass Loss Test (NAMLT) Specimen Preparation

Specimens were prepared in accordance with ASTM G67, measuring 50 mm by 6 mm by the actual material thickness. The as-received specimens were machined down to 6.35 mm (0.25 inch) thickness to match the shipboard plate thickness; see Figure 19 (b).

C. CHARACTERIZATION TECHNIQUES

1. Optical Microscope

A Nikon Epiphot 200 optical microscope was used for imaging, shown in Figure 20. The microscope is capable of magnifications of x25, x100, x200, x500, and x1000. It was used to determine rolling direction of the specimens so test specimens could be prepared according to the applicable ASTM specifications.

Figure 20. Nikon Epiphot 200 Optical Microscope

2. Scanning Electron Microscope (SEM)

A Zeiss Neon 40 field emission SEM, shown in Figure 21, was used to determine grain size, grain orientation, and grain boundary precipitate morphology and distribution. Secondary and backscatter electron images were captured with backscatter diffraction (BSD) being the primary mode of characterization at energies between 15 and 20 keV, with up to 1.32×10^{-6} mA beam current and a working distance of approximately 6.5 millimeters.

Figure 21. Zeiss Neon 40 Field Emission SEM

3. Energy Dispersive Spectroscopy (EDS)

An EDAX Pegasus EDS analysis system is mounted on the Zeiss SEM described above. It was used to verify chemical composition of the material met AA5456 specifications and to distinguish β-phase precipitate from the Al-Mg matrix. Elemental spectra were collected at 20KV with a $1.32x10^{-6}$ mA beam current.

4. Electron Backscatter Diffraction (EBSD)

EBSD was used to determine grain orientation and grain boundary continuity. Grain boundary β-phase continuity is an indicator of the degree of sensitization: continuous (sensitized), partially continuous (partially sensitized), and discontinuous (not sensitized). Images were captured at 20KV with a $1.32x10^{-6}$ mA beam current, using a working distance of 11 to 12 millimeters at a 70-degree tilt.

5. Nitric Acid Mass Loss Test (NAMLT)

NAMLT was conducted to quantitatively determine the degree of sensitization of all specimens, which is correlated to the degree of intergranular corrosion susceptibility. Test specimens were contained in a beaker filled with

400 mL, 70 wt% nitric acid. Temperature was controlled by a Digi-Sense temperature controller and thermocouple connected to a Glas-Col 380 Watt heating element (Figure 22). Specimens were weighed on a Sartorius model CP225D digital scale (Figure 23).

The β-phase precipitate is anodic to the surrounding Al-Mg solution. It is preferentially corroded by the nitric acid, resulting in a loss of mass or the grain boundary precipitate. Using the test apparatus shown in Figure 21, test specimens were immersed in nitric acid for 24 hours, with temperature maintained at 30°C (86°F). Specimens were weighed and the total surface area determined before and after the test. The resulting loss in mass indicates the degree of sensitization. According to ASTM G67 a mass loss greater than 25 mg/cm^2 is susceptible to intergranular corrosion, which can lead to stress corrosion cracking [14].

Figure 22. NAMLT Apparatus

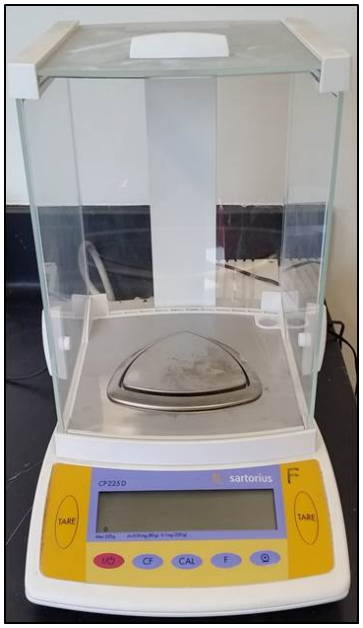

Figure 23. Sartorius Model CP225D Digital Scale

6. Tensile Test

Tension tests were conducted on an Instron model 4507 using Bluehill software (Figure 24). The apparatus employed wedge-type grips. Specimens were subjected to constant extension rate until they failed, using a cross-head speed of 1 mm/minute. Load-elongation data were reduced to engineering stress versus engineering plastic strain curves. Engineering 0.2% offset yield strength values were used to determine whether the reverse sensitized specimens' yield strength was within specifications for in service use outlined in ASTM B928 Standard Specification for High Magnesium Aluminum—Alloy Sheet and Plate for Marine Service and Similar Environments [1]. As-received and shipboard sensitized specimens were tested for comparison.

Figure 24. Instron Model 4507

7. Corrosion Test

Stress corrosion cracking thresholds (K_{1scc}) of sensitized and reverse sensitized AA5456 were measured by L. Raymond and Associates [13]. Experimental test procedures were developed for testing sensitized aluminum using ASTM F1624 Standard Test Method for Measurement of Hydrogen Embrittlement Threshold in Steel by the Incremental Step Load Technique as guidance [19].

III. RESULTS AND DISCUSSION

A. OPTICAL MICROSCOPE

1. Results

In this case, the optical microscope was used to determine the rolling direction of the Al-Mg plates so test specimens could be fabricated in the appropriate orientation. These images are of relatively low quality because they capture an unprepared surface. The surfaces were intentionally left unprepared so the as-fabricated rolling direction was readily visible. All results were similar to those shown in Figure 25.

Figure 25. Rolling Direction Determination

2. Discussion

Using this information, NAMLT and tensile test specimens were prepared with the rolling direction parallel to the longitudinal dimension of the test specimens, according to ASTM G67 [14] and B557M [18]. SEM specimens were also fabricated in longitudinal and transverse rolling directions, with the majority of their images captured in the longitudinal direction, which better displayed grain boundary precipitate continuity.

Material properties vary in each direction, particularly a strain hardened material in question. An anisotropic material's elongated grain boundaries influence the impact of IGC leading to SCC. The orientation that material is tested has shown to have critical effect on various test results [8], [20]. Therefore, care was taken to identify rolling direction prior to any specimen preparation.

B. SEM

1. Results

Micrographs were collected of as-received, in-service (shipboard), known sensitized, and heat treated specimens. These images are shown in Figures 26 through 29.

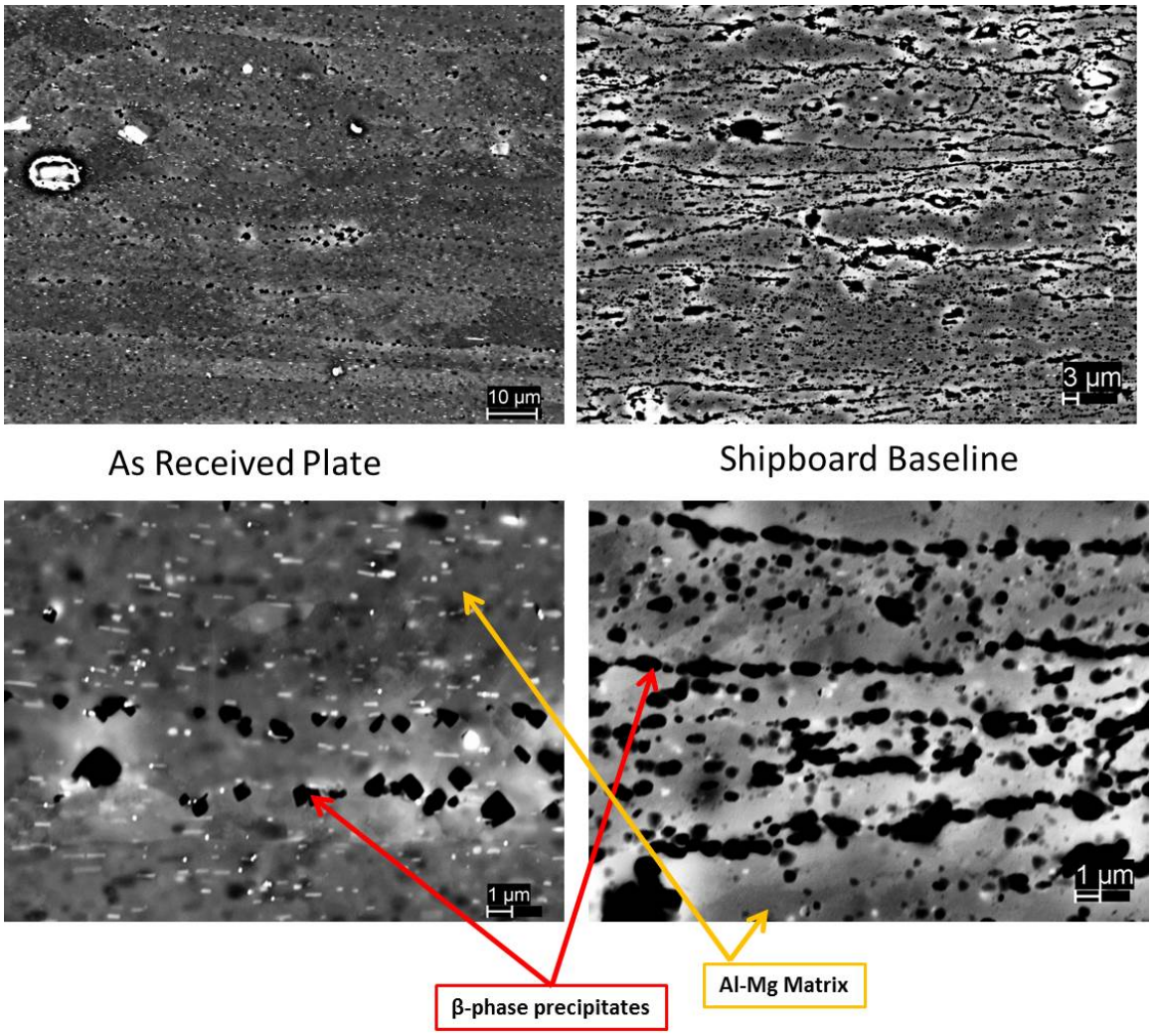

Figure 26. SEM Backscatter Images of As-received and In-service (Shipboard) Plates (Obtained by Electron Backscatter Detector)

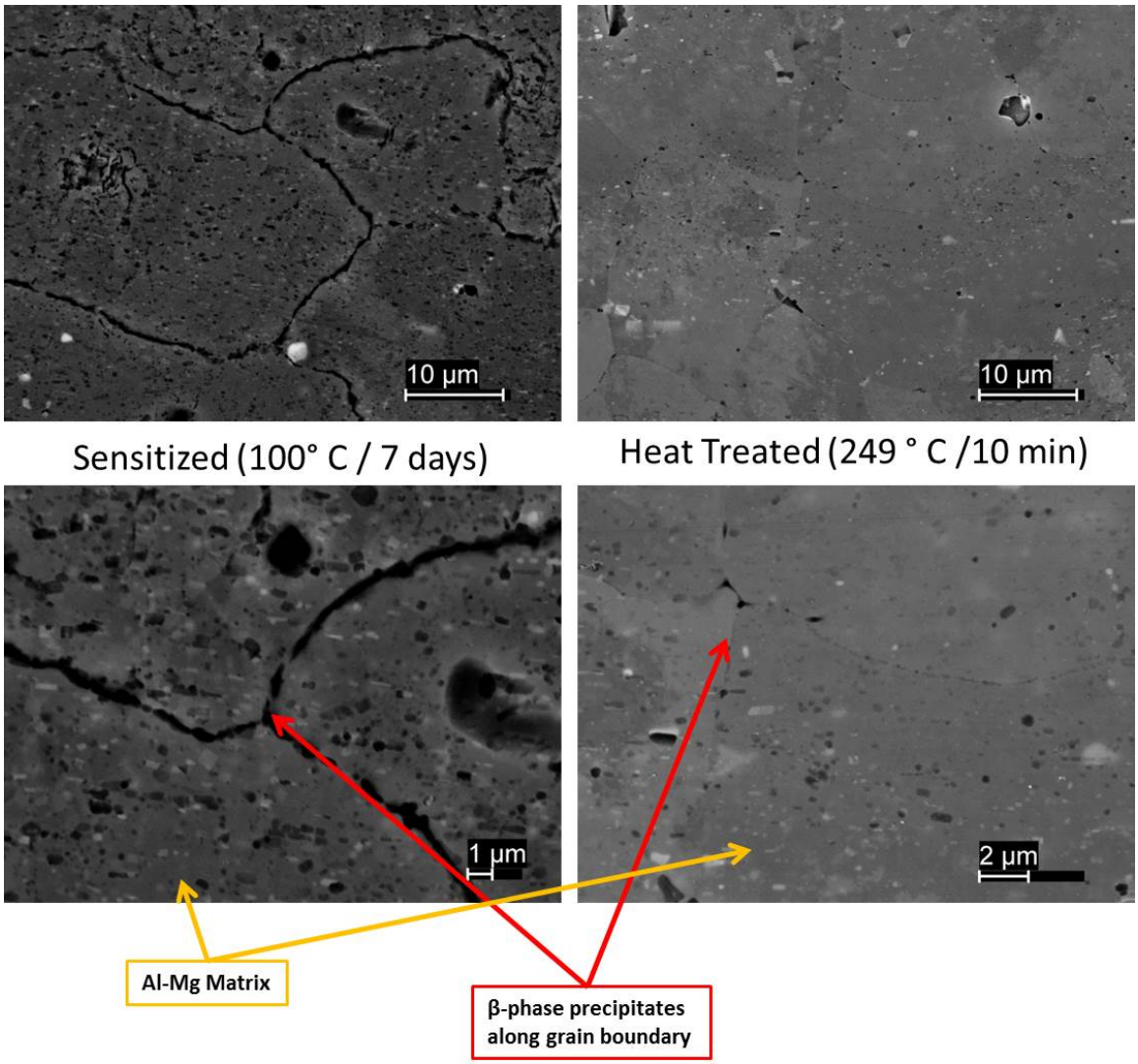

Figure 27. SEM Backscatter Images of Sensitized and Heat Treated AA 5456-H116 (Obtained by Electron Backscatter Detector)

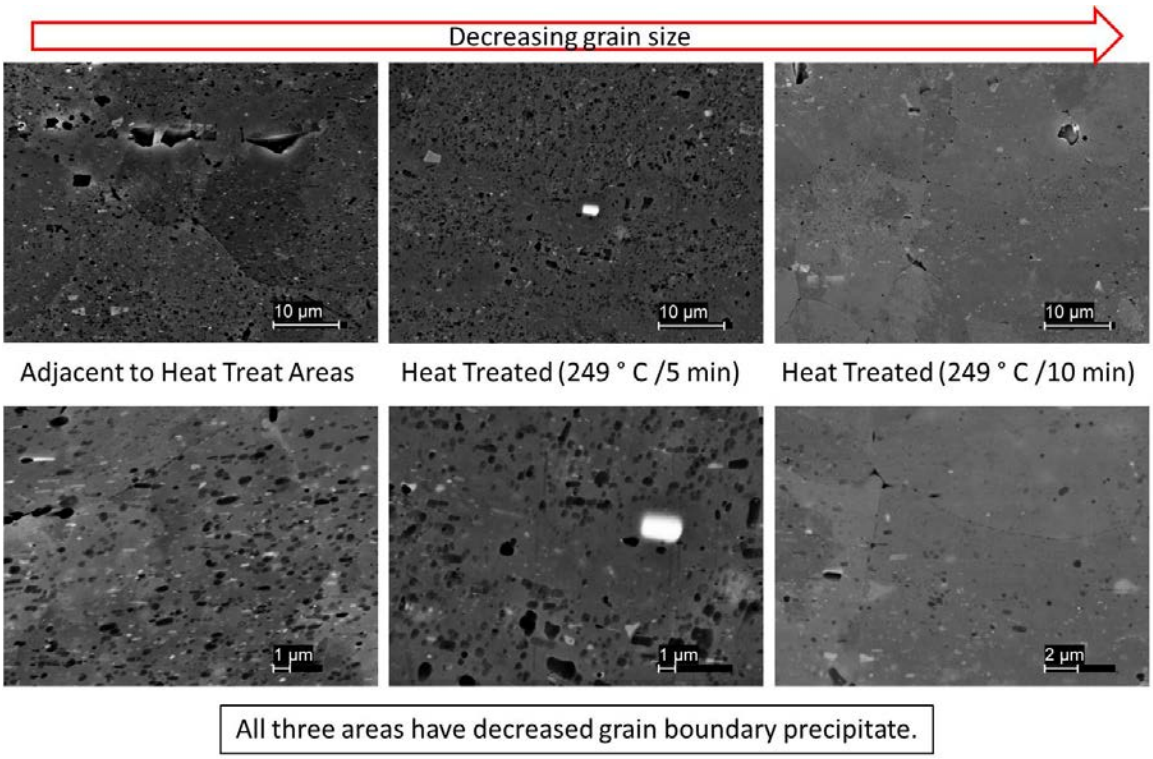

Figure 28. SEM Backscatter Images of Heat Treatment Profiles
(Obtained by Electron Backscatter Diffraction)

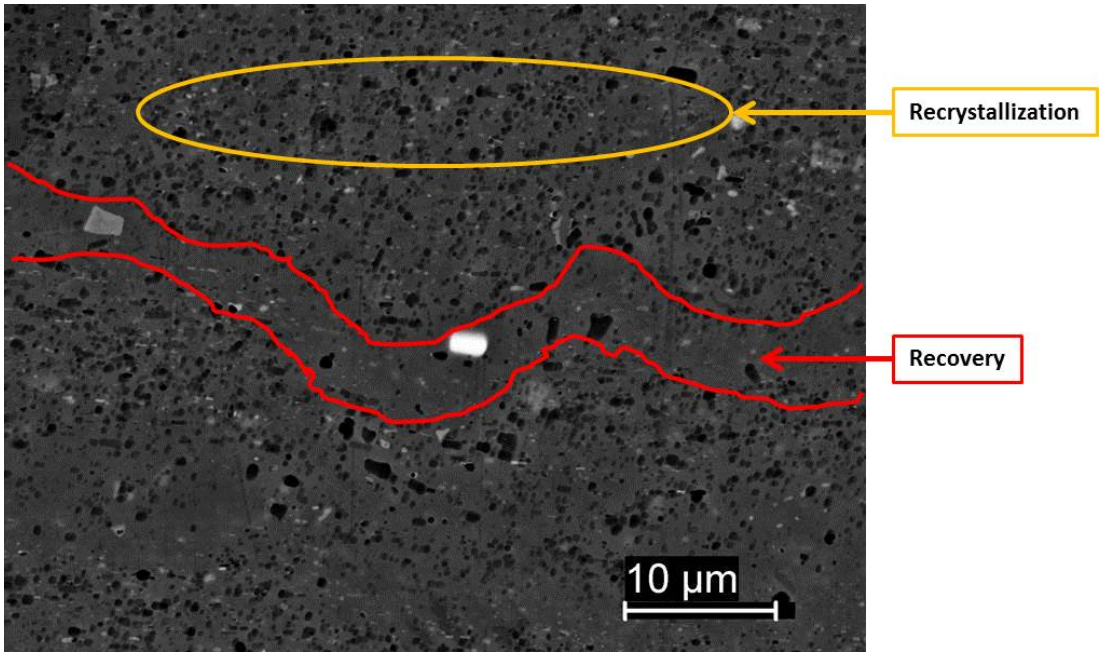

Figure 29. SEM Backscatter Image of 249°C / 5 Minute Profile
(Obtained by Electron Backscatter Detector)

2. Discussion

Two things are evident in Figure 26. First, the as-received plate has discontinuous grain boundary precipitation. Secondly, the shipboard plate does have more grain boundary β-phase precipitate but, again, the grain boundary precipitates are not continuous, indicating that this material is also partially sensitized.

A comparison of sensitized and heat treated microstructures is shown in Figure 27. The sensitized specimen has a continuous β-phase at grain boundaries indicative of a fully sensitized material. The applied heat treatment clearly reversed sensitization as indicated by reduction of grain boundary precipitate. The 10-minute profile is shown here, but the 5-minute treatment had a similar reduction in grain boundary precipitate, as did the adjacent material not intentionally subjected to heat treatment. Aluminum is a very thermally conductive material. As such, the applied heat treatments also reverse sensitized adjacent material because of the conducted heat.

Kramer et al. explored whether an induction heat treating system would result in adjacent material becoming re-sensitized as a result of this nuisance heating [9]. They found that adjacent material was not re-sensitized by 200 °C and 240 °C held for one hour, as shown in Figure 10. Although the adjacent material could experience annealing, there is little risk that it will be re-sensitized as a result of induction heat treatment applied to adjacent areas.

All three areas from the heat-treated plate are shown in Figure 28. Aside from showing a reduction in grain boundary precipitate in all cases, each also show evidence of annealing compared to microstructures from Figure 26. The as-received and non-sensitized shipboard specimens have exhibit elongated grains as expected in a strain hardened (rolled) microstructure. The microstructures shown in Figure 28 exhibit equiaxed grains, which suggests the material was recrystallized by the heat treatment. As shown in Figure 29, the 5-minute profile contains areas where recovery and recrystallization are evident.

The temperature and time required for annealing is dependent on the percent of alloying Mg, and on the degree of strain hardening of the material. This relationship is described in Figure 9, which identifies the annealing temperature to be around 250 °C for an alloy containing 5% Mg [9]. In another study by Koizumi et al., a 5% Mg material in a strain hardened condition and subsequently heated for 5 minutes at 250 °C resulted in about 50% recrystallization [21]. This would be about the same profile as the 249 °C/ 5 min heat treat that produced the microstructure in Figure 29.

AA5456-H116 is strain hardened by cold rolling during manufacture. The H116 temper treatment is performed to prevent grain boundary precipitate [11]. Both Oguocha et al. and Davenport et al. found that rolled material with low-angle grain boundaries were more SCC resistant than material with high-angle boundaries [7], [11]. Grain boundary precipitation along the high-angle boundaries will lead to greater susceptibility to SCC as a result [7].

C. EDS

1. Results

EDS chemical composition analysis was conducted of all specimens and compared to AA5456 specifications contained in Table 1. In AA5456, Mg is the major alloying element. It is added for strength. Higher Mg content results in increased strength of Al-Mg alloys. The maximum solid solubility in aluminum is 17.4 wt%; however the Mg content of commercially available alloys does not exceed 5.5 wt. % due to concerns with sensitization [1]. Other alloying elements are included in smaller amounts with their purposes also listed in Table 1.

Table 1. Chemical Composition of 5xxx series Al-Mg Alloys. Adapted from [6], [22].

Alloy	Si	Fe	Cu	Mn	Mg	Cr	Zn	Ti	Zr
5052	0.25	0.4	0.1	0.1	2.2-2.8	0.15-0.35	0.1	-	xx
5059	0.45	0.5	0.25	0.60-1.2	5.0-6.0	0.25	0.40-0.90	0.2	xx
5083	0.4	0.4	0.1	0.40-1.0	4.0-4.9	0.05-0.25	0.25	0.15	xx
5086	0.4	0.5	0.1	0.20-0.70	3.5-4.5	0.05-0.25	0.25	0.15	xx
5383	0.25	0.25	0.2	0.7-1.0	4.0-5.2	0.25	0.4	0.15	xx
5454	0.25	0.4	0.1	0.50-1.00	2.4-3.0	0.05-0.20	0.25	0.2	xx
5456	0.25	0.4	0.1	0.50-1.00	4.7-5.5	0.05-0.20	0.25	0.2	xx
6005A	.50-.90	0.35	0.3	0.5	.40-.70	0.3	0.2	0.1	xx
6061	.40-.80	0.7	.15-.40	0.15	.80-1.20	0.04-0.35	0.25	0.15	xx
6063	0.20-0.60	0.35	0.1	0.1	0.45-0.90	0.1	0.1	0.1	xx
6082	0.7-1.3	0.5	0.1	0.40-1.0	0.6-1.2	0.25	0.2	0.1	xx
Alloy Purpose	Formbility, Corrosion Resistance	Strength	Machinability, Corrosion Resistance	Formability, Strength	Strength	Strength, Corrosion Resistance	Strength	Strengh, High Melting Temp.	Corrosion Resistance

a. As-received (Non-sensitized) AA5456

Shown in Table 2, EDS chemical composition of as-received plate measured 92.15 wt % Al, 5.24 wt % Mg, and lesser amounts of Si, Ti, Cr, Mn, Fe, Cu, and Zn that were within specifications for AA5456. Secondary electron image and EDS spectrum for this sample are shown in Figures 30 and 31.

Table 2. Chemical Composition of As-received AA5456 (Obtained by EDS)

Element	Wt%	At%
MgK	05.24	05.86
AlK	92.15	92.85
SiK	00.03	00.03
TiK	00.29	00.17
CrK	00.40	00.21
MnK	00.92	00.45
FeK	00.27	00.13
CuK	00.28	00.12
ZnK	00.41	00.17

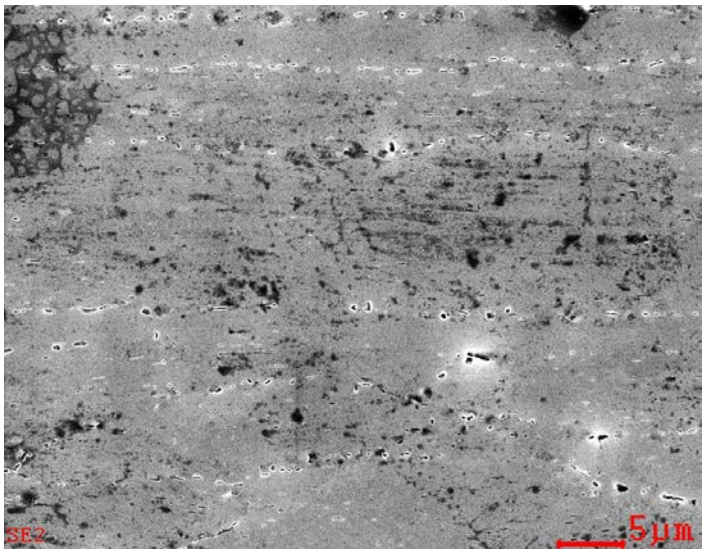

Figure 30. Secondary Electron Image of As-received AA5456

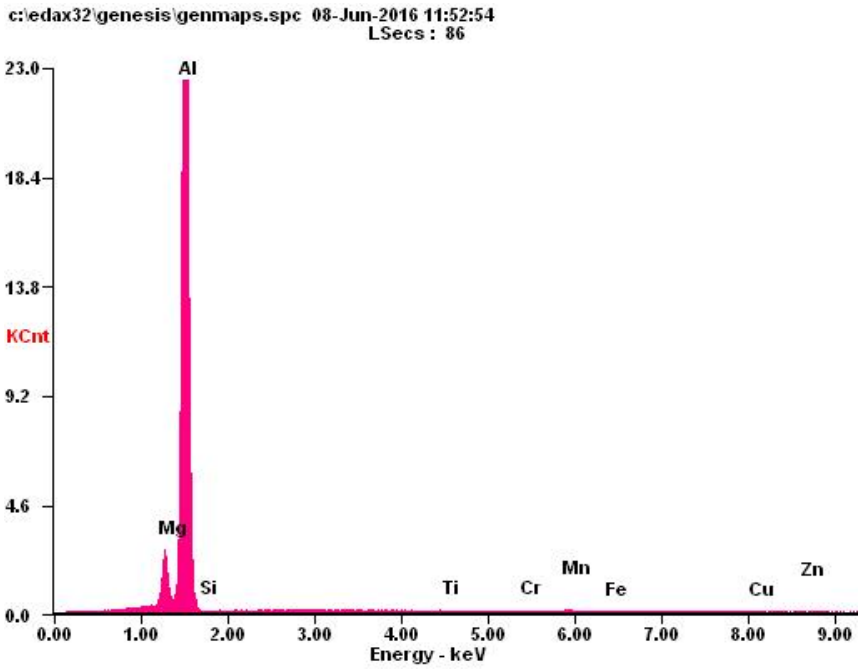

Figure 31. EDS Spectrum of As-received AA5456

b. Shipboard AA5456

Shipboard sourced plates exhibited a similar chemical composition, but did have slightly higher Mg content than the 5.5 wt% specified. Results are

shown in Table 3, and Figures 32 and 33. Of note, the image in Figure 32 contains features resembling “worms.” These features were found to be artifacts of the polishing/etching process and are not a feature of the material.

Table 3. Chemical Composition of Shipboard AA5456
(Obtained by EDS)

Element	Wt%	At%
MgK	05.84	06.51
AlK	91.88	92.35
SiK	00.03	00.03
TiK	00.33	00.19
CrK	00.38	00.20
MnK	00.76	00.38
FeK	00.31	00.15
CuK	00.26	00.11
ZnK	00.20	00.08

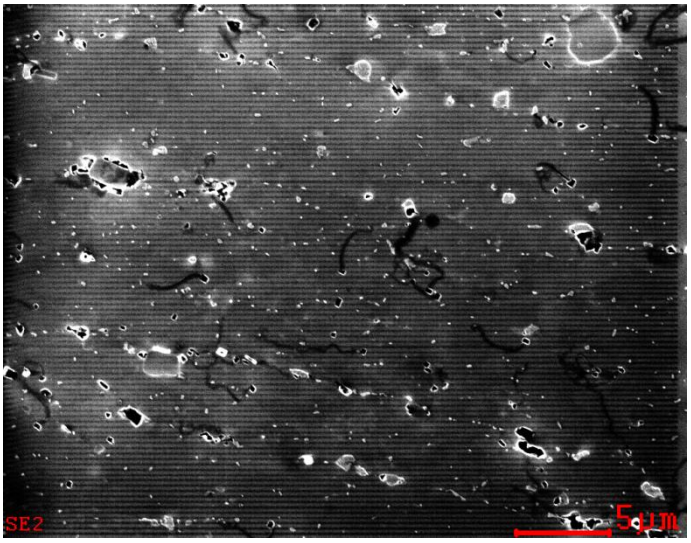

Figure 32. Secondary Electron Image of Shipboard AA5456

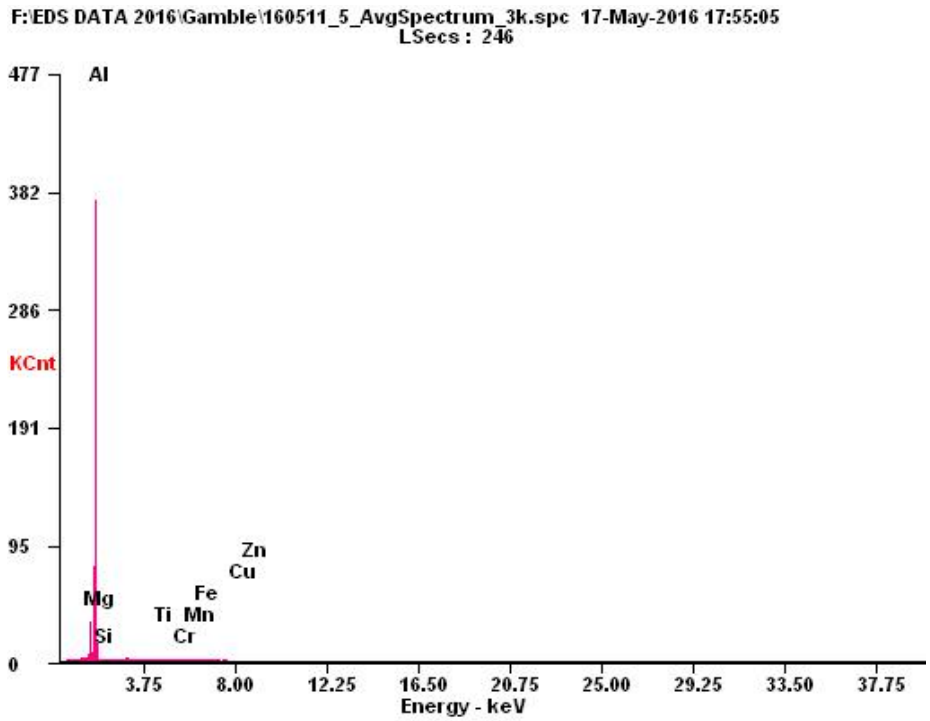

Figure 33. EDS Spectrum of Shipboard AA5456

c. Heat Treated AA5456

The heat treated plate also contained the correct Mg wt% for AA5456. Major elemental constituents are shown in Table 4. Only Al and Mg are shown in this table, as there were not significant peaks of other elements. Elemental distribution varies depending on the exact spectrum location. This plate includes both heat treatment profiles and adjacent material.

Table 4. Chemical Composition of Heat Treated AA5456

Element	Wt%	At%
MgK	05.15	05.68
AlK	94.85	94.32
Matrix	Correction	ZAF

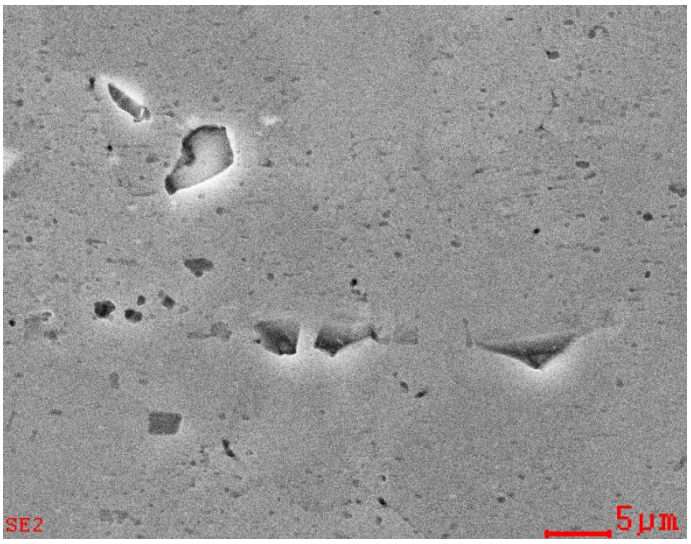

Figure 34. Secondary Electron Image of Heat Treated AA5456

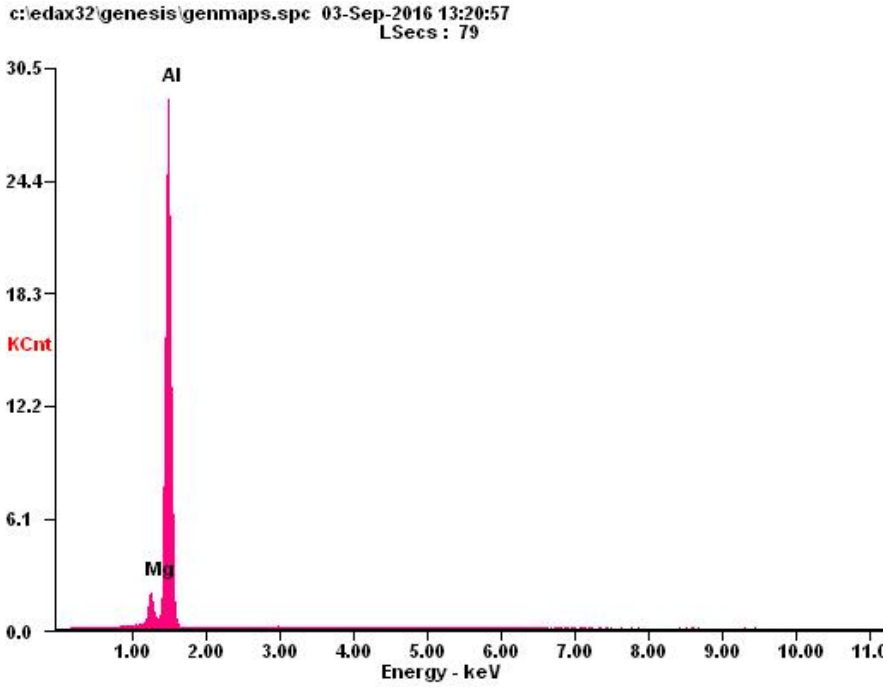

Figure 35. EDS Spectrum of Heat Treated AA5456

d. Elemental Mapping

EDS elemental mapping was conducted, but results were not consistent and were therefore not ultimately used for material characterization purposes.

The goal of this technique was to discern Mg rich β-phase precipitates from the surrounding Al-Mg matrix. While some β-phase precipitates were identified, they were largely indistinguishable from the Al-Mg matrix. In Figure 36, the grain boundary area shows a dispersed Mg concentration, but it does more finely identify Fe-Mn particles. Fe is a strength additive, while Mn provides corrosion resistance [22].

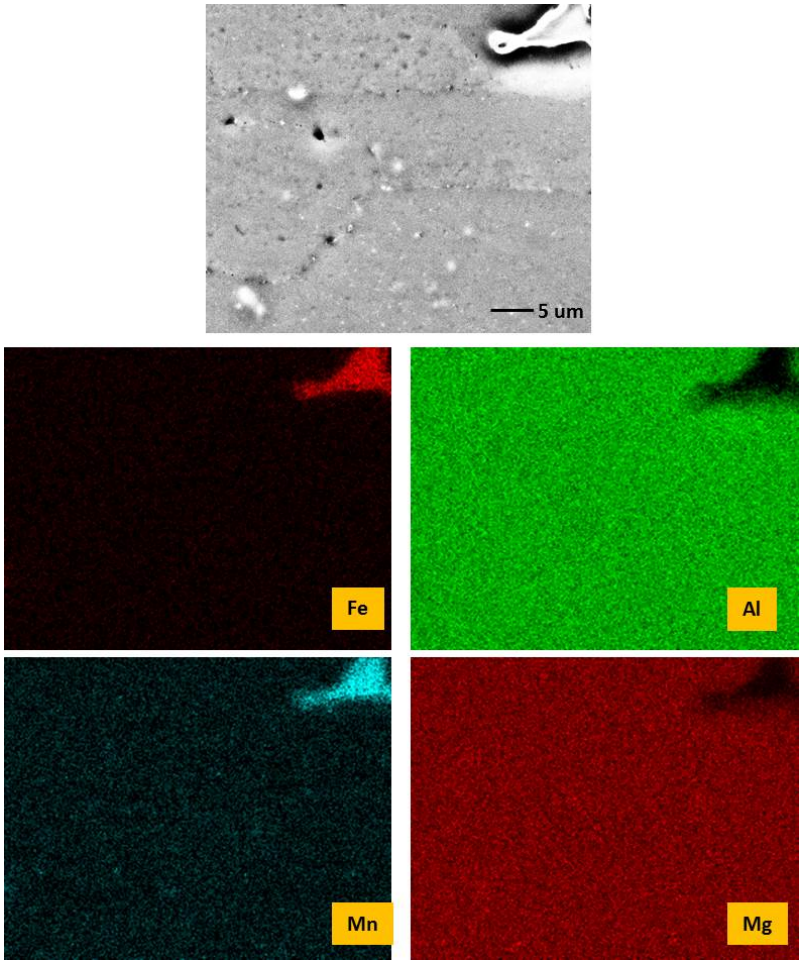

Figure 36. Elemental Map of As-received AA5456

2. Discussion

There are two possible reasons why EDS elemental mapping may not have produces the desired data. The size of the β-phase precipitates ($Al_3Mg_{2)}$ is 25–100 nm. The resolution of the EDS beam is 1 µm (1000 nm). Thus, the resolution of SEM based EDS is not a good match for this material. Also, the electro-polishing and etching of relatively soft Al-Mg removed particles from the surface, including the β-phase precipitate that is the target. The location of grain boundary precipitate is still visible, but we are likely viewing the location of the precipitate before it was removed by polishing and etching. A future area of study in this field should include elemental mapping with a transmission electron microscope (TEM) with a higher resolution.

The heat treatment process had no effect on the elemental composition. Mg content did vary among the different plates, but this could be attributed to material being sourced from different manufacturers at various times.

D. EBSD

1. Results

EBSD scans were conducted on as-received and shipboard plates. In Figures 37 and 38, the images on the left have the Al-Mg matrix represented by the colored area and the grain boundary areas represented by the dark areas. The images on the right are mirror images, with colored grain boundaries and dark Al-Mg matrix. Grain boundary orientation is listed in the bar graphs as a percentage of grains at low to high angles.

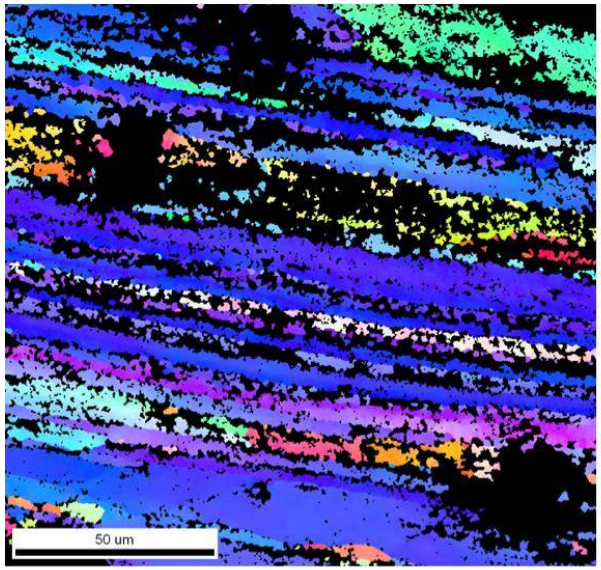

Colored areas: Al-Mg matrix
Dark areas: Grain boundary precipitates

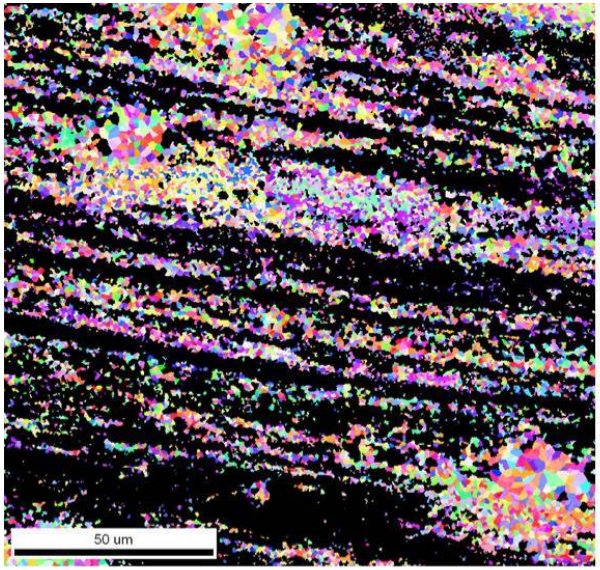

Dark areas: Al-Mg matrix
Colored areas: Grain boundary precipitates

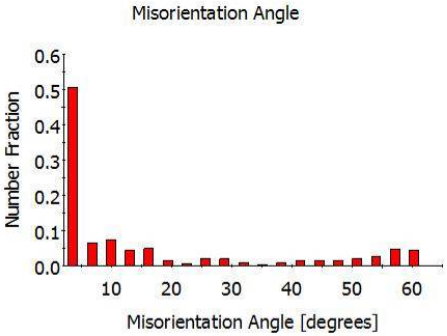

Figure 37. EBSD Scan of As-received AA 5456

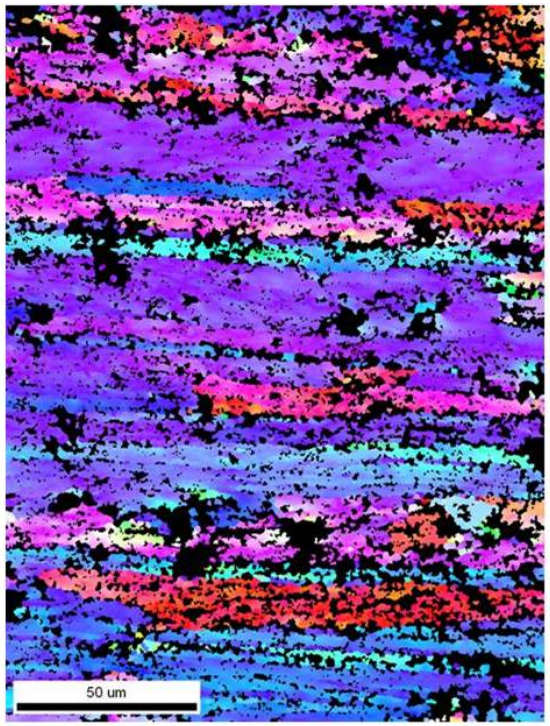

Colored areas: Al-Mg matrix
Dark areas: Grain boundary precipitate

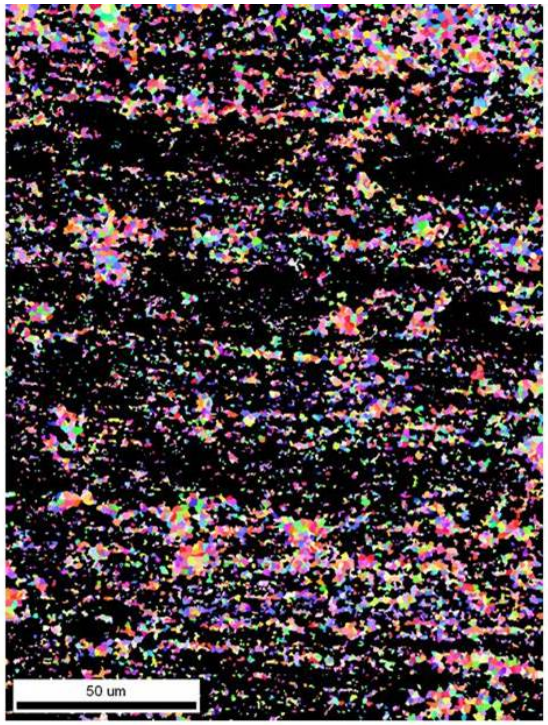

Dark areas: Al-Mg matrix
Colored areas: Grain boundary precipitate

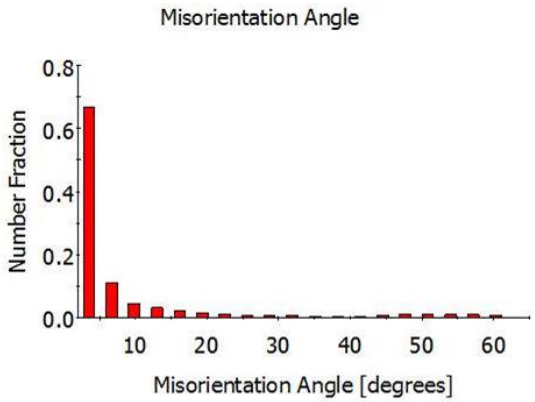

Figure 38. EBSD Scan of Shipboard AA 5456

2. Discussion

In both of the EBSD scans shown in Figures 37 and 38 we see grains elongated in the rolling direction, with a high fraction of low angle boundaries. Elongated grains are a result of the cold rolling process during manufacture. Strain hardening by rolling increases material strength and hardness due to the plastic deformation.. Rolled AA5456 will tend to have low grain boundary misorientations anglesdue to recovery within the elongated grains resulting from the rolling process. Low-angle grain boundaries are resistant to β-phase precipitation, and resistant to SCC as a result [7], [11].

Material with low-angle boundaries will tend to have greater strength than annealed, coarse-grained material. According to the Hall-Petch relationship, finer grains will provide greater resistance to slip than coarser grains although the role of grain boundary misorientation has not been fully resolved [22]. More resistance to slip will result in higher ultimate tensile strength (UTS) and yield strength.

Crystallographic indexing of cubic beta phase posed problems due to partial loss of the particles during the polishing process, and thus not accurate. A comparison of Figures 37 and 38 leads to a confusing conclusion. The as-received plate appears to have more grain boundary precipitate than the shipboard plate. This information contradicts backscatter images and NAMLT results. It was surmised that EBSD could not provide expected results in this case. Therefore, EBSD scans were not ultimately used to draw conclusions in this research.

Had EBSD scans been conducted on the heat treated material, their grain structure was expected be less directional but with coarser grains and higher angle grain boundaries due to the observed recrystallization. At above 1/% Mg recrystallization is accelerated, and even more so in rolled alloys due to the stored energy of high dislocation densities as a result of rolling [21].

EBSD scans can determine grain and grain boundary orientation and composition under different test conditions. It is recommended that future EBSD work use more careful material preparation techniques – i.e., polishing and etching techniques that do not remove grain boundary precipitate yet still produces a surface quality allowing high magnification microscopy.

E. NAMLT

1. Results

NAMLT results are shown in Table 5. According to ASTM G67 [14], a mass loss of 1–15 mg/cm^2 indicates a material that is IGC resistant, while a mass loss of 25–75 mg/cm^2 indicates a material that is IGC susceptible.

Table 5. NAMLT Results

Specimen	Source description	Mass Loss (mg/cm^2)
NS1	As-received	4.36
NS2	As-received	4.41
3A1	Active ship	7.35
3A2	Active ship	5.80
6A1	Active ship	12.62
6A2	Active ship	11.83
Sensitized	Active ship	72.50
Sensitized	Active ship	75.80
H5-1	Heat treated 249 °C/5 min	8.13
H5-2	Heat treated 249 °C/5 min	6.15
H10-1	Heat treated 249 °C/10 min	5.18
H10-2	Heat treated 249 °C/10 min	3.54
Adjacent-1	Active ship	3.38
Adjacent-2	Active ship	2.72
Adjacent-3	Active ship	5.37
Adjacent-4	Active ship	3.34
Adjacent-5	Active ship	2.82
Adjacent-6	Active ship	2.84

2. Discussion

These results indicate that specimens from as-received, “3A” and “6A” plates are IGC resistant. These results were expected in the as-received plate, but were not expected in the shipboard plates (3A and 6A). Plates 3A and 6A did have a mass loss higher than the as-received plate, indicating that the sensitization process had begun. SEM images also agree that they are partially sensitized by comparing grain boundary continuity in Figure 26.

Both the 5- and 10-minute heat treatment profiles reduced the mass loss of the sensitized plate to “IGC resistant” levels. The 10-minute profile performed slightly better. These results confirm SEM observations that β-phase precipitate returned to solution, reversing sensitization. The results also make sense considering the temperature range at which the β-phase should return to solution, as viewed in the phase diagram in Figure 6 [12]. Mg concentrations between 3% and 5% correspond with a 150 °C to 250 °C range to return Mg to solution. As these samples are around 5.5%, the 249 °C heat treatment temperature was an intuitive choice. The material adjacent to the targeted heat treatment areas was similarly affected. This suggests that the heat treatment process did not precisely target the intended area and because of aluminum’s high thermal conductivity surrounding areas were also affected. The adjacent material mass loss agrees with the SEM observations above.

F. TENSILE TEST

1. Results

Tensile test results were compared to AA 5456-H116 specifications outlined in ASTM B928M, Standard Specification for High Magnesium Aluminum Alloy Sheet and Plate for Marine Service and Similar Environments [1]. Minimum tensile strength and yield strength are 315 MPa and 230 MPa, respectively. [18] The minimum yield strength is the metric for comparison as it is more useful for material that is not designed to yield in service. For welded material, yield

strength is also a more accurate measurement of material strength following welding heat cycles.

Raw test data was exported from Bluehill software into comma separated value (.csv) format. The measured load and change in specimen length were used to calculate engineering stress and strain according to the equations in Figure 39. The machine stiffness was removed from the curve by performing linear regression of the elastic region and subtracting points that did not correspond to the tested material's modulus of elasticity. The resulting plots display the material's Engineering Plastic Strain (Tables 6–9 and Figures 40–43).

$$Stress = \frac{Force}{Area}$$

$$Strain = \frac{Final\ Length - Original\ Length}{Original\ \ Length}$$

Figure 39. Stress-Strain Equations

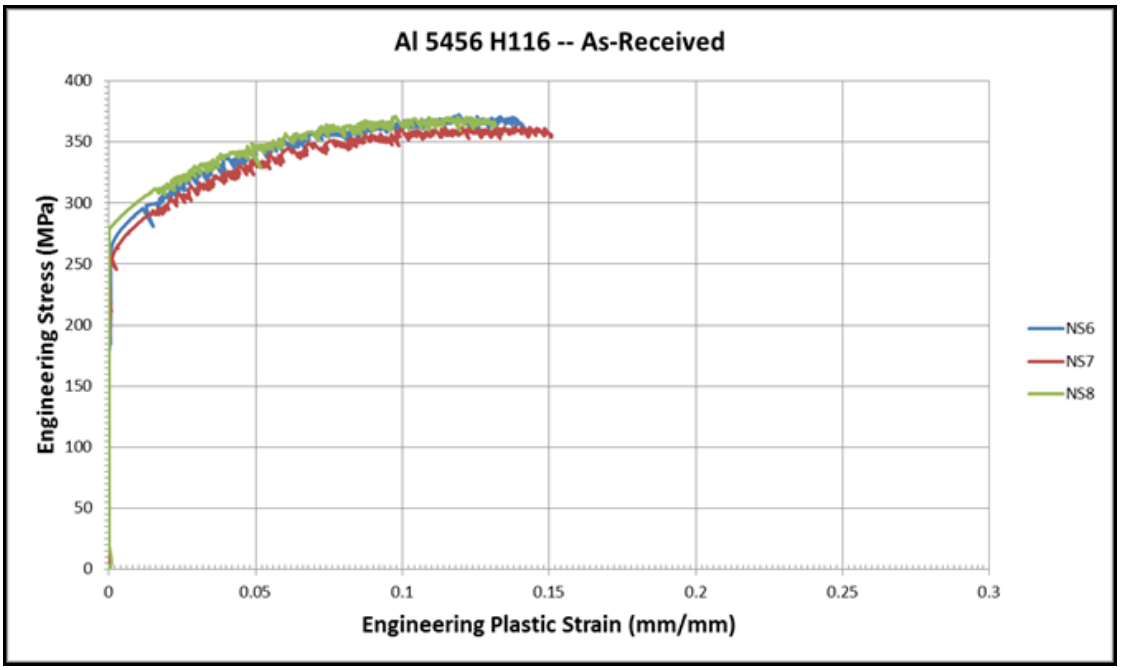

Figure 40. As-received AA 5456 Stress Strain Curve

Table 6. As-received AA 5456 Tensile Test Results

	UTS (MPa)	YS (MPa)
N6	373	271
N7	363	261
N8	371	284
Avg	369	272

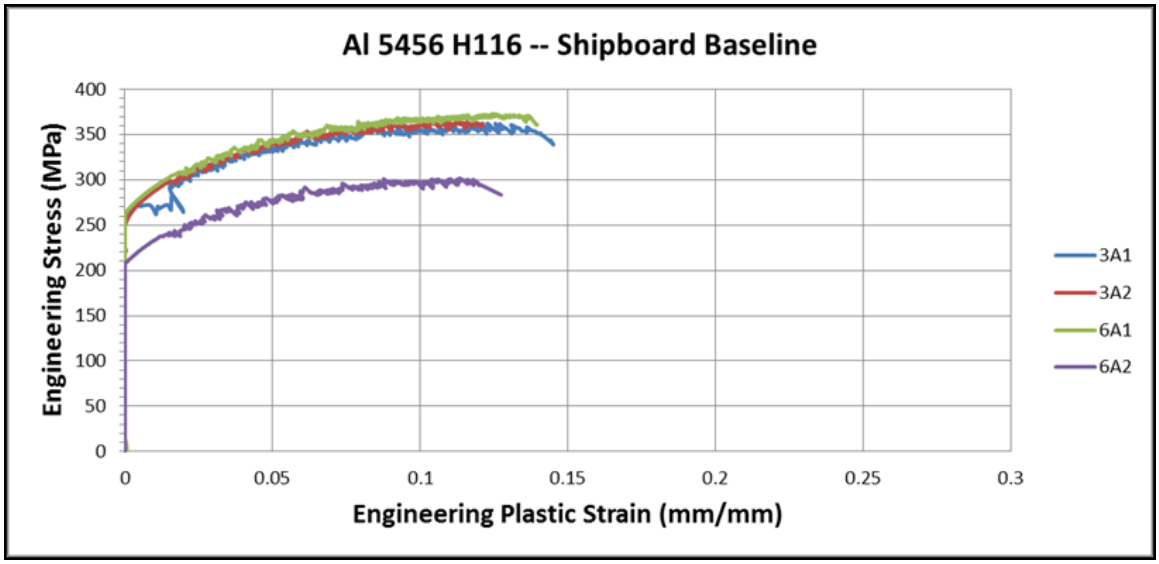

Figure 41. Shipboard Baseline AA 5456 Stress Strain Curve

Table 7. Shipboard Baseline AA 5456 Tensile Test Results

	UTS (MPa)	YS (MPa)
3A1	362	269
3A2	364	236
6A1	373	272
6A2	302	212
Avg	350	247

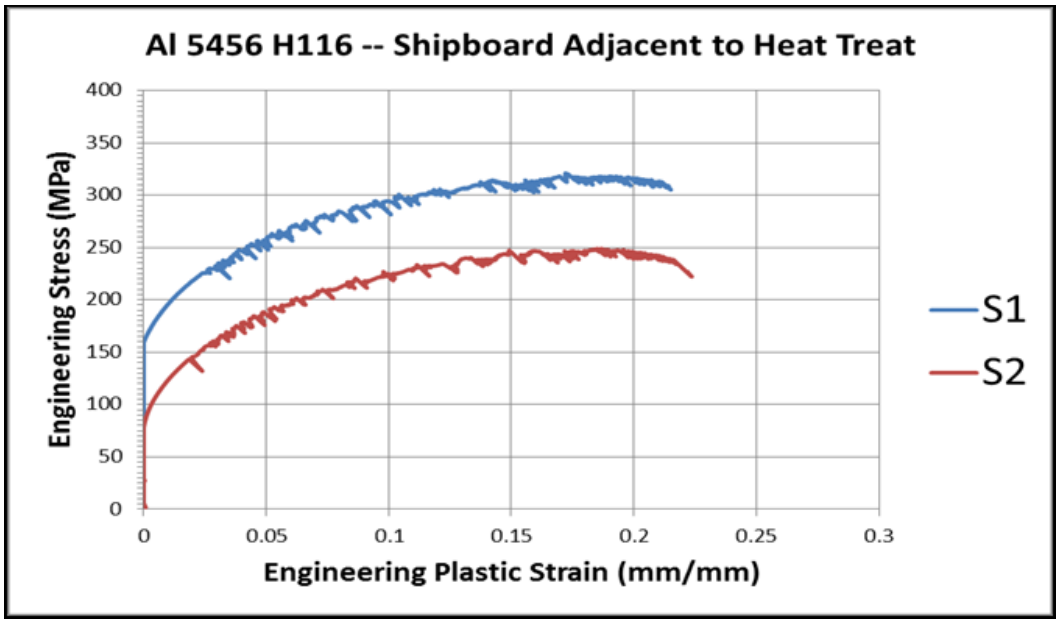

Figure 42. Adjacent AA 5456 Stress Strain Curve

Table 8. Adjacent AA 5456 Tensile Test Results

	UTS (MPa)	YS (MPa)
S1	321	169
S2	249	94
Avg	285	132

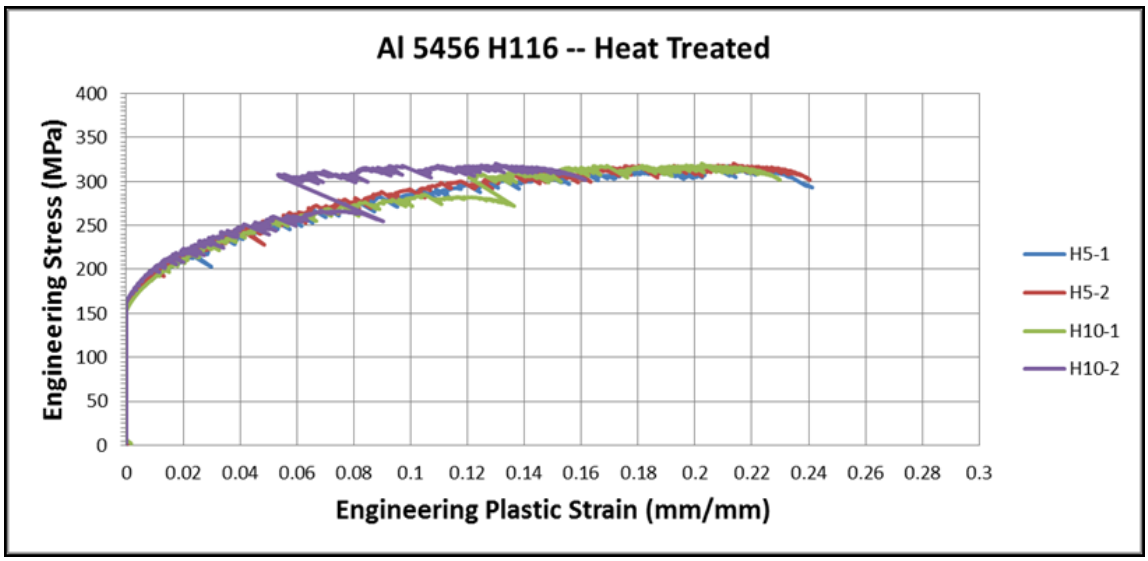

Figure 43. AA5456 Heat Treated 249 °C/5 Min Stress Strain Curve

Table 9. AA5456 Heat Treated 250 °C/5 Min Tensile Test Results.

	UTS (MPa)	YS (MPa)
H5-1	317	173
H5-2	321	169
H10-1	321	164
H10-2	321	174
Avg	320	170

2. Discussion

The as-received specimens met ASTM B928 [1] specifications for yield strength. The shipboard baseline material is also, on average, within specification although these specimens have greater variability in their results compared to as-received specimens. All of the specimens from the heat treated plate were below 230 MPa yield strength, with the lowest yield strength being from the material adjacent to the targeted heat treatments. The heat treated specimens were also more ductile. Having a lower yield strength and higher ductility is a result of the material being annealed by heat treatment. This is consistent with the annealing temperatures in Figure 9 [9] and the work conducted by Koizumi et al. [21]. It could also be an effect of having been in service while sensitized. As Mg precipitates from solution, the matrix loses some alloy strengthening gained through Mg in solid solution, resulting in lower mechanical properties [11].

These results show that it is possible that induction heat treatment can be effective in reversing sensitization, but should be applied to material whose yield strength is within an acceptable value, like those in Figures 40 and 41. Additional tests should be performed on the same plate through a reverse sensitization process to verify the heat treatment is annealing the material, resulting in a loss of strength. In other tensile tests conducted by NSWC-CD, in-service AA5456 was tested in the sensitized and non-sensitized states [23]. These results agree closely with shipboard in-service AA5456 yield stress ranging from 224 to 284 MPa. Sensitized AA5456 in their test, however, had slightly higher yield stress; around 189 MPa compared to 170 MPa for the heat treated AA5456 and

132 MPa for the material adjacent to the heat treated area. This does suggest that material properties may have been lost during the heat treatment, but other variables such as different in-service lifetimes, different material batches, and different residual stresses could explain some of the yield strength loss. The use of sub-sized specimens could also explain overall lower material strength in these tests. According to ASTM B557M, paragraphs 6.14 and 6.1.6, the use of sub-sized specimens may not correspond to tests of full size specimens [18]. Sub-sized specimens were used due to the limited amount of material on hand to test.

Another noteworthy result is that yield strength was affected by sensitization much more than UTS. As Mg comes out of solution to form β-phase precipitate, less Mg is in the matrix to provide the solid solution strengthening as designed. Yield strength is affected more because, as plastic deformation occurs during tension testing, dislocations multiply and the material again becomes strain hardened up to fracture [22]. This is also reflected in the "saw tooth" pattern of the plastic region, shown in Figures 40 through 43.

Both of the 10-minute heat treatment specimens' stress strain curves shown in Figure 43 have a pronounced "jump" in the middle of the their plastic region. This was considered an artifact of the tests due to those specimens experiencing failure at the gauge section and into the test specimen grip section.

G. CORROSION TEST

1. Results

Complete test report provided by L. Raymond and Associates [13] summarized as follows:

- For sensitized AA 5456 in the T-L orientation, K_{1scc} was equal to 15.6 MPa√m (14.2 ksi√in) with a fast fracture strength, K_{1c} equal to 25.8 MPa√m (23.5 ksi√in).

- For desensitized AA 5456 in the T-L orientation, K_{1scc} was equal to 24.1 MPa√m (21.9 ksi√in) with a fast fracture strength, K_{1c} equal to 24.6 MPa√m (22.4 ksi√in).

2. Discussion

A low K_{1scc} indicates the value that will initiate crack propagation due to SCC [22]. It is compared here to K_{1c} that indicates the value that will initiate crack propagation due to a material flaw in a benign environment (i.e. not seawater). K_{1scc} will naturally be lower than K_{1c} and is the fracture strength of concern for marine applications. K_{1scc} of the desensitized (reverse sensitized) AA5456 is in line with expected fracture toughness for aluminum alloys [24].

Results show that the reverse sensitization of AA 5456 by heat treatment restores the SCC threshold to the material, verifying the heat treatment process as a viable way to desensitize (reverse sensitize) material and restore its resistance to SCC.

THIS PAGE INTENTIONALLY LEFT BLANK

IV. CONCLUSIONS

This research considered various AA5456-H116 samples in various stages of sensitization and in-service use. Several characterization techniques were used to determine the microstructure, yield strength, degree of sensitization, elemental composition, grain boundary conditions, and SCC thresholds. Materials were characterized in the sensitized and reverse sensitized conditions to determine the efficacy of in-situ induction heat treatment to reverse sensitization.

Both the 5- and 10-minute heat treatment profiles successfully reversed sensitization, with no clear distinction as to which performed better. In both cases micrographs and NAMLT data agree that β-phase grain boundary precipitate was dissolved into solution, lowering the degree of sensitization. The surrounding material not intentionally targeted with heat treatment was also affected, indicating the process did not precisely target the intended treatment area. Evidence of recrystallization can be seen in micrographs, suggesting that substantial annealing had occurred.

The yield strength of heat treated material was below the minimum specification for AA5456-H116. This may have been attributed to the material's prolonged service life in the sensitized condition, but may have been a result of annealing due the high temperature of the heat treatment. The reverse sensitized material did experience restoration of its SCC threshold, indicating that it could return to service if other material properties were also in specification.

In all, the heat treatment time and temperatures profiles considered were partially successful. While both profiles did successfully reverse sensitization and restore SCC threshold values, they may have annealed the material which negatively affected the yield strength and the resulting microstructure.

THIS PAGE INTENTIONALLY LEFT BLANK

V. FUTURE WORK

a. EBSD

Although EBSD techniques were not successful during this research, this technique could be used for future work. Specimen preparation was the most difficult part of this thesis paper. Too little surface preparation, specifically etching, resulted in images with no visual value. Too much etching resulted in good visual quality, but the process of etching removed the β-phase precipitates from the surface. A dedicated study could seek the ideal material surface conditions and the EBSD scan settings to properly use EBSD as a characterization technique in this context. If material preparation is perfected, the resolution needs to be around 25 nm to distinguish the β-phase precipitate (Al_3Mg_2) from the surrounding AlMg matrix.

b. STEM EDS elemental mapping

Another characterization technique to use is Scanning Transmission Electron Microscopy (STEM) EDS elemental mapping. The results of SEM characterization from this research are qualitative. To study the β-phase volume fraction quantitatively requires greater resolution then SEM EDS provides. Due to the additional material preparation time required for STEM characterization, this technique was not used for this paper. Future work that does not also include a wide range of mechanical property research could focus on quantitative elemental analysis of sensitized and reverse sensitized Al-Mg alloy.

c. Analyze close to sensitization/stabilization boundary

The heat treatment profile in studied in this paper (249°C) is near the stabilization/anneal boundary shown in Figure 44. A comparison could be made between lower heat treatment temperatures that are closer to the sensitization/stabilization boundary. If reverse sensitization is performed at lower temperatures and maintains a similar microstructure to higher temperature

reverse sensitized material this would be an advantage for increased efficiency of in-situ reverse sensitization.

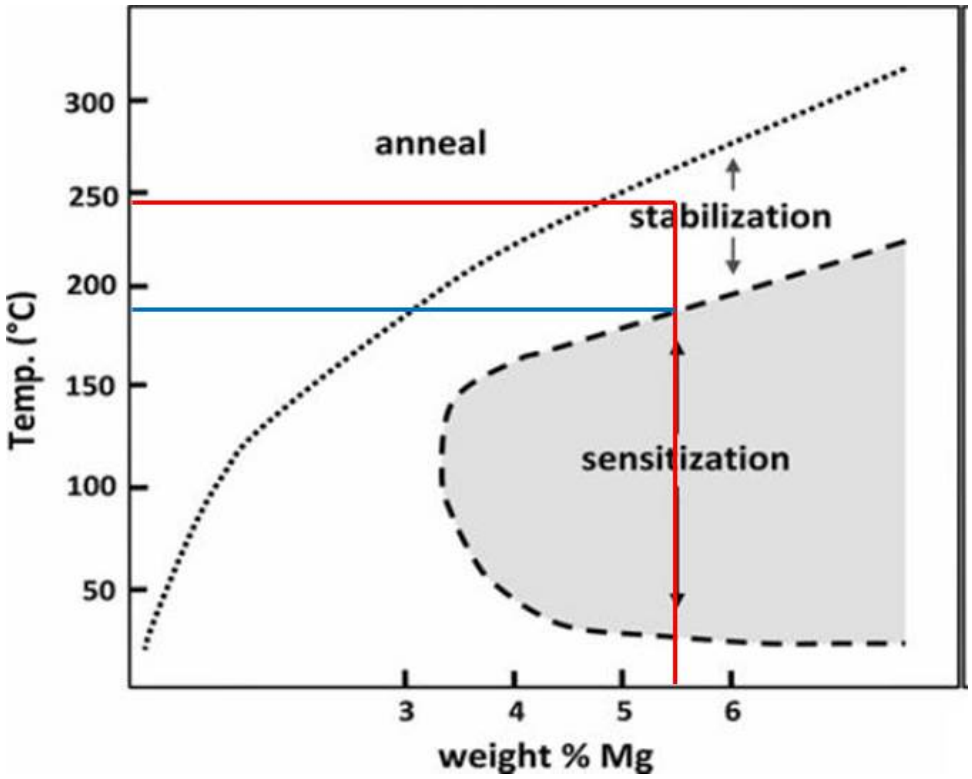

Figure 44. Effect of Temperature on Al-Mg Alloys. Adapted from [9].

d. Other heat treatment techniques – high power diode laser (HPDL) arrays

Because the ultimate goal driving this technology is in situ reverse sensitization of ship hulls and superstructures, the heat treatment equipment used needs to be both highly portable and finely controlled. In addition to the induction system used for this paper, other types of systems should be studied. An example of anther heat treating technology is light emitting diode (LED) arrays. These arrays were designed to pre- and post- heat steels during friction stir welding [25] and may be suited for heating Al-Mg alloys in the context of this study. LED arrays can be finely tuned and controlled with computer based

software. They are also scalable, making them suitable for small to large areas. This scalability also makes them portable – a large array can be assembled on site.

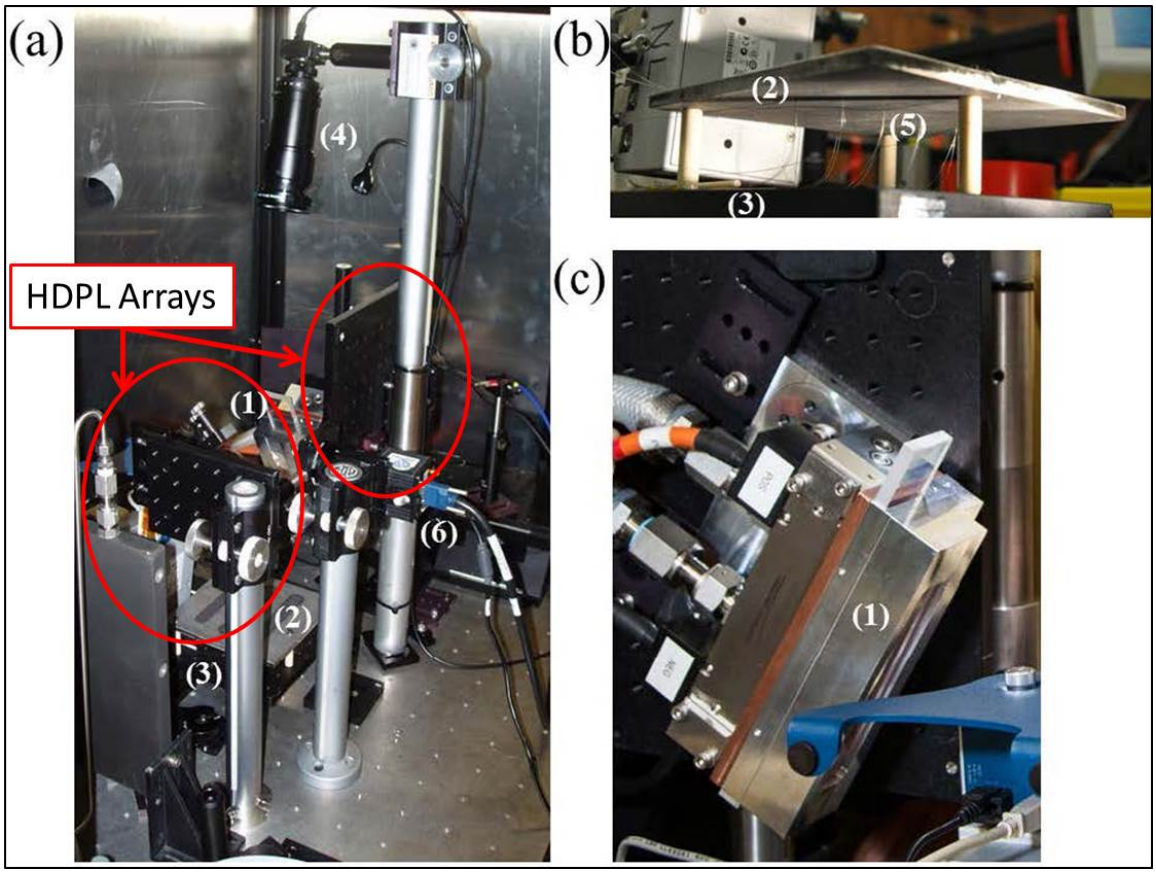

(a) Full view showing all components, (b) close up view of workpiece, thermocouples, and stage, and (c) close up view of the HPDL array. Component numbering: (1) HDPL array, (2) HY-80 workpiece, (3) moving stage, (4) CCD camera, (5) thermocouples, and (6) IR camera.

Figure 45. HDPL Array. Adapted from [25].

e. Determine optimal in-service time to treat

Material studied in this research displayed a lower yield strength after being placed into service. Successfully reverse sensitized material could still be precluded from returning from service due to inadequate yield strength. A topic of study that should be considered is the determination of the proper in-service time

to apply a reverse sensitization heat treatment. The goal would be to employ the treatment *before* the material's strength was degraded. There would also be a clear determination whether the material is annealed by the treatment.

LIST OF REFERENCES

[1] ASTM International, ASTM B928/B928M: *Standard Specification for High Magnesium Aluminum-Alloy Sheet and Plate for Marine Service and Similar Environments*, West Conshohocken: ASTM International, 2009.

[2] J. C. Benedyk, "International temper designation systems for wrought aluminum alloys: Part I—strain hardenable (H temper) aluminum alloys," *Light Metal Age*, October, pp. 26–30, 2009.

[3] K. N. Tran, “Stress Corrosion Cracking in 5XXX (Al-Mg) alloys” (Classroom presentation), presented at Monterey, CA, 2016.

[4] K. N. Tran, "aluminum alloys corrosion mitigation technologies reverse sensitization” (Slide Briefing), Naval Surface Warfare Center, Carderock Division, West Bethesda, 2015.

[5] Eric F. Herzberg, "The Annual cost of Corrosion for Army Ground Vehicles and Navy Ships," LMI Government Consulting, Tysons, 2006.

[6] R. Sielski, *Ship Structure Committee-452: Aluminum Structure Design and Fabricatin Guide*, Washington, DC: United States Coast Guard, 2007.

[7] A. J. Davenport, Y. Yuan, R. Ambat, B. J. Connolly, M. Strangwood, A. Afseth and G. Scamans, "Intragranular corrosion and stress corrosion cracking of sensitized AA5182," *Materials Science Forum*, vols. 519–521, July, pp. 641–646, 2006.

[8] R. G. Kelley, *Development and Validation of an Integrated Intergranular Corrosion/Cracking Model*, Arlington: Office of Naval Research, 2007.

[9] L. Kramer, "Locally reversing sensitization in 5xxx aluminum plate," *Journal of Materials Engineering and Performance*, vol. 21, no. 6, pp. 1025–1029, 2012.

[10] E. C. Cormack, “The effect of sensitization on the stress corrosion cracking of aluminum alloy 5456,” M.S. thesis, Dept. of Mech. Eng., Naval Postgraduate School, Monterey, CA, 2012.

[11] I. N. A. Oguocha, O. J. Adigun and S. Yannacopoulos, "Effect of sensitization heat treatment on properties of Al–Mg alloy," *Journal of Material Sciences,* vol. 43, no. Online Issue, pp. 4208-4214, 2008.

[12] ASM International, "Alloy Phase Diagrams Center," [Online]. Available: http://www1.asminternational.org.libproxy.nps.edu/asmenterprise/apd/default.aspx. [Accessed 17 July 2016].

[13] L. Raymond and Associates, "LRA Report: NAVSEA'14-1205 (Comparison of KIscc of Sensitized and Desensitized Aluminum Alloy 5456 in the T-L and L-T Orientations)," L. Raymond and Associates, Newport Beach, 2015.

[14] ASTM International, ASTM G67: Standard test method for determining the susceptibility to intergranular corrosion of 5XXX series aluminum alloys by mass loss after exposure to nitric acid (NAMLT test), West Conshohocken: ASTM International, 2004.

[15] US Navy Chief of Information, "United States Navy fact file," 13 January 2016. [Online]. Available: http://www.navy.mil/navydata/fact_display.asp?cid=4200&tid=800&ct=4. [Accessed 15 August 2016].

[16] USCarriers.net, "USS Monterey (CG 61)," [Online]. Available: http://www.uscarriers.net/cg61history.htm. [Accessed 15 August 2016].

[17] ASTM International, ASTM E399: Standard practice for making and using precracked double beam stress corrosion specimens, West Conshohocken: ASTM International, 2009.

[18] ASTM International, ATSM B557M: Standard test methods fortension testing wrought and cast aluminum- and magnesium-alloy products (metric), West Conshohocken: ASTM International, 2015.

[19] ASTM International, ASTM F1624: Standard test method for measurement of hydrogen embrittlement threshold in steel by the incremental step loading technique, West Conshohocken: ASTM International, 2012.

[20] F. Bovard, "Development of test specimens for evaluating SCC behavior," in *NACE Corrosion Conference and Expo*, Houston, 2011.

[21] M. Koizumi, "Kinetics of recrystallization in Al-Mg alloys," *Zeitschrift fur Metallkunde,* vol. 91, no. 6, pp. 460–467, 2000.

[22] W. D. Callister and D. G. Rethwisch, *Materials Science and Engineering an Introduction*, Hoboken: John Wiley and Sons, 2009.

[23] Westmoreland Mechanical Testing and Research, Inc., "Report number 6-37802," Youngstown: Westmoreland Mechanical Testing and Research, Inc., 2006.

[24] M. Meyers and K. Chawla, in *Mechanical Behavor of Materials*, Cambridge, UK: Cambridge University Press, 2009, p. 848.

[25] B. Baker et. al, "Use of High-Power diode Laser Arrays for Pre- and Post-Weld Heating During Friction Stir Welding of Steels," in *Friction Stir Welding and Processing VIII*, Hoboken, NJ: Wiley, 2015.

THIS PAGE INTENTIONALLY LEFT BLANK

INITIAL DISTRIBUTION LIST

1. Defense Technical Information Center
   Ft. Belvoir, Virginia

2. Dudley Knox Library
   Naval Postgraduate School
   Monterey, California